Inorganic Chemistry

Article

pubs.acs.org/IC

Tuning the Reactivity in Classic Low-Spin d^6 Rhenium(I) Tricarbonyl Radiopharmaceutical Synthon by Selective Bidentate Ligand Variation (*L,L′*-Bid; *L,L′*= *N,N′*, *N,O*, and *O,O′* Donor Atom Sets) in *fac*-$[Re(CO)_3(L,L'\text{-Bid})(MeOH)]^n$ Complexes

Marietjie Schutte,[†] Gerdus Kemp,[†,‡] Hendrik G. Visser,*[,†] and Andreas Roodt*[,†]

[†]Department of Chemistry, University of the Free State, P.O. Box 339, Bloemfontein 9300, South Africa

[‡]Department of Chemistry, University of Johannesburg, Auckland Park 2006, South Africa

Supporting Information

ABSTRACT: A range of *fac*-$[Re(CO)_3(L,L'\text{-Bid})(H_2O)]^n$ (*L,L′*-Bid = neutral or monoanionic bidentate ligands with varied *L,L′* donor atoms, *N,N′*, *N,O*, or *O,O′*: 1,10-phenanthroline, 2,2′-bipydine, 2-picolinate, 2-quinolinate, 2,4-dipicolinate, 2,4-diquinolinate, tribromotropolonate, and hydroxyflavonate; *n* = 0, +1) has been synthesized and the aqua/methanol substitution has been investigated. The complexes were characterized by UV−vis, IR and NMR spectroscopy and X-ray crystallographic studies of the compounds *fac*-$[Re(CO)_3(Phen)(H_2O)]NO_3\cdot 0.5Phen$, *fac*-$[Re(CO)_3(2,4\text{-dQuinH})(H_2O)]\cdot H_2O$, *fac*-$[Re(CO)_3(2,4\text{-dQuinH})Py]Py$, and *fac*-$[Re(CO)_3(Flav)(CH_3OH)]\cdot CH_3OH$ are reported. A four order-of-magnitude of activation for the methanol substitution is induced as manifested by the second order rate constants with (*N,N′*-Bid) < (*N,O*-Bid) < (*O,O′*-Bid). Forward and reverse rate and stability constants from slow and stopped-flow UV/vis measurements (k_1, M^{-1} s^{-1}; k_{-1}, s^{-1}; K_1, M^{-1}) for bromide anions as entering nucleophile are as follows: *fac*-$[Re(CO)_3(Phen)(MeOH)]^+$ (50 ± 3) × 10^{-3}, (5.9 ± 0.3) × 10^{-4}, 84 ± 7; *fac*-$[Re(CO)_3(2,4\text{-dPicoH})(MeOH)]$ (15.7 ± 0.2) × 10^{-3}, (6.3 ± 0.8) × 10^{-4}, 25 ± 3; *fac*-$[Re(CO)_3(TropBr_3)(MeOH)]$ (7.06 ± 0.04) × 10^{-2}, (4 ± 1) × 10^{-3}, 18 ± 4; *fac*-$[Re(CO)_3(Flav)(MeOH)]$ 7.2 ± 0.3, 3.17 ± 0.09, 2.5 ± 2. Activation parameters ($\Delta H^{\ddagger}_{k1}$, kJmol^{-1}; $\Delta S^{\ddagger}_{k1}$, J K^{-1} mol^{-1}) from Eyring plots for entering nucleophiles as indicated are as follows: *fac*-$[Re(CO)_3(Phen)(MeOH)]^+$ iodide 70 ± 1, −35 ± 3; *fac*-$[Re(CO)_3(2,4\text{-dPico})(MeOH)]$ bromide 80.8 ± 6, −8 ± 2; *fac*-$[Re(CO)_3(Flav)(MeOH)]$ bromide 52 ± 5, −52 ± 15. A dissociative interchange mechanism is proposed.

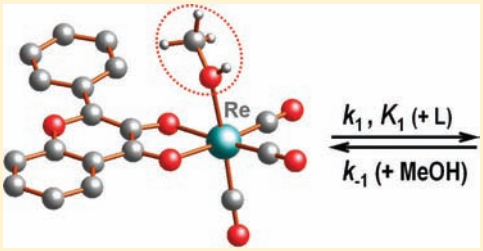

INTRODUCTION

Significant interest has been shown over the past decade or more in rhenium and technetium complexes, bearing the *fac*-$[M(CO)_3]^+$ entity (M = Tc(I), Re(I)), as potential diagnostic and therapeutic radiopharmaceuticals, respectively. The application thereof for the treatment of cancer was spearheaded by and has to be credited to a large extent to Alberto et al.[1−6] Characteristics which render complexes of the type *fac*-$[M(CO)_3(H_2O)_3]^+$ so attractive for application in nuclear medicine are the inert *fac*-$[M(CO)_3]^+$ core, from classic crystal field considerations, and the relative labile water molecules bound to it. It is no wonder then that several promising compounds have been synthesized in the past few years by employing these tricarbonyl synthons by linking it to biomolecules as target director systems.[7−12]

There are however a number of aspects that have to be considered for radiopharmaceutical design. Ideally, the preparation must be a one-step synthesis, the final purity must be very high (preferably 98% yield), the biomolecule concentration should be 1:1 in respect to the radionuclide and the time required for the synthesis, and therefore the half-life of the radionuclide utilized, are important considerations. In principle, these limitations translate to the following: any preparation has to be performed in saline solution (0.9% NaCl in water or buffer), and no purification should be needed. Thus radiolabeled compounds should have a very high specific activity when addressed for receptor targeting and the preparation should not exceed a certain time; in the case of ^{99m}Tc, it is only 60 min.

The above limitations make it clear why the introduction of organometallic compounds into radiopharmacy was rather unattractive until recently. Since the labeling of a biomolecule with *fac*-$[M(CO)_3(H_2O)_3]^+$ (M = Re, ^{99m}Tc) requires the substitution of at least one water ligand, the upper limit is therefore the water self-exchange rate in the complex itself. This is a crucial factor and makes it possible to predict if the labeling of a biomolecule will occur with a reasonable rate and if it will be convenient in practice. The first thermodynamic and kinetic data for water exchange on *fac*-$[Re(CO)_3(H_2O)_3]^+$ was obtained by Salignac and co-workers by using a variety of NMR techniques.[13] The positive $\Delta S^{\ddagger}$ value of +14(10) J K^{-1} mol^{-1} obtained for this process suggested an I_d mechanism. The possibility of dissociative activation was further supported by

Received: June 28, 2011
Published: November 23, 2011

   dx.doi.org/10.1021/ic2013792 | *Inorg. Chem.* 2011, 50, 12486−12498

the fact that the rate of water exchange was similar to water substitution rates for a range of entering ligands ranging from neutral N and S donors to halides.

Similar studies on other rhenium and technetium compounds have been described.[14−20] These addressed different aspects of the reaction mechanism associated with these species and indicated that the activation process on anation reactions in the protonated forms of the $[MO_2(CN)_4]$ type of complexes proceed via assumed different intimate mechanisms, depending on which site is considered.[21−27]

Activation volumes, $\Delta V^{\ddagger}$, were obtained for S and N bonded ligands[28,29] and ranged from slightly negative (S bonded ligands) to slightly positive (N), indicating a shift from I_a for the S ligands to I_d for the N ligands. It was reasoned that the mechanism of substitution was affected by the fact that the harder N donor ligands made discrimination between water and entering ligands more difficult than for the better nucleophiles (S ligands).

The slower water exchange rates observed for *fac*-$[Re(CO)_3(H_2O)_3]^+$ as compared to the similar reactions for Tc(I) does not exclude it totally as a potential radionuclide. The main reasons for this are first that the reactions of Re complexes could be studied as models for the similar Tc complexes and second that the effect of ligands other than the coordinated CO ligands (e.g., different bidentates) on the rate of aqueous substitution has not yet been investigated. There are only a few structures of complexes of the form *fac*-$[Re(CO)_3(L')(L)(H_2O)]^n$ (L and L′ = neutral mono- or bidentate N-bonded ligands) in the literature. Interestingly, the Re(I)−OH_2 bond distances vary substantially, in spite of the similarity in the N-bonded ligands. Re(I)−OH_2 distances vary from 2.190(5) Å for *fac*-$[Re(CO)_3(Bipy)(H_2O)]CF_3SO_3$ and 2.181(5) Å for *fac*-$[Re(CO)_3(Phen)(H_2O)](NO_3)0.5(CF_3SO_3)0.5.H_2O$ to the much shorter distances reported for different guanine complexes (2.168(4) and 2.167(4) Å).[30] Moreover, in the case of *N,O*-Bid ligands to yield neutral Re(I) complexes, there seem to be quite a variation in bond distances (as long as 2.198(5) Å) in spite of the similarities in ligand types.[31−33] At a first glance the Re−OH_2 bond seems to be longer for *fac*-$[Re(CO)_3(H_2O)_3]^+$ (2.201(14) Å)[34] than for most of the *fac*-$[Re(CO)_3(L')(L)(H_2O)]^n$ complexes, although the uncertainty in the bond length needs to be taken into account. Be as it may, the reason for this is unclear as one would expect the opposite, but it definitely underlines the necessity for more crystal structure data in order to better understand the possible labilization of the Re−OH_2 bond by bidentate ligands. For this reason, we initiated a crystallographic study and report here four representative crystal structures to illustrate the synthesis of the aqua, coordinated methanol or mono-ligated complexes.

The potential that complexes of the general form *fac*-$[Re(CO)_3(L,L'\text{-Bid})(H_2O)]^n$ (*L,L*′-Bid = neutral or monoanionic bidentate ligands, n = 0, +1) could be activated therefore exists and might be efficient for potential use in radiopharmacy, especially considering the [2 + 1] mixed ligand approach proposed by Alberto et al.[35] An extensive kinetic study of the effect of bonded ligands on the reactivity of normally inert Re(I)−tricarbonyl complexes, as classic low-spin d^6 complexes, is considered essential for the possible use of this synthon in radiopharmacy, either as a diagnostic or as a therapeutic tool. This clearly will contribute toward predicting for example, time required to do proper labeling of director ligand systems, as well as predicting stabilities of labeled complexes. For this reason, as second part of this study, we selected a range of complexes with systematically varied bidentate ligands and donor atoms and evaluated the lability and mechanism of substitution of the 'labile site', occupied by a coordinated aqua/methanol ligand by simple monodentate nucleophiles. Although the coordination compounds have in many cases been isolated as the aqua complexes, these were all converted to the corresponding MeOH complexes upon dissolution in methanol for the kinetic studies, due to solubility limitations in water. We thus report here the first comprehensive kinetic study of coordinated methanol substitution reactions in *fac*-$[Re(CO)_3(L,L'\text{-Bid})(MeOH)]^n$ [*L,L*′-Bid: *N,N*′-Bid (1,10-phenantroline, 2,2′-bipyridine); *N,O*-Bid (2-picolinate, 2-quinolinate, 2,4-pyridinedicarboxylate, 2,4-Quinolinedicarboxylate); *O,O*′-Bid (tribromotropolonate and 3-hydroxyflavonate)] with a representative number of monodentate entering nucleophiles, ranging from halides to pyridines and S and P donor groups, with supporting X-ray diffraction data to fully characterize starting complexes and products.

The choice of bidentate ligands was a conscious one to afford complexes with a positive (*N,N*′-Bid ligands) or neutral charge (*N,O*-Bid and *O,O*′-Bid), with varied Bronsted basicities as manifested by the corresponding pK_a values for the *L,L*′-BidH ligands, which are as follows: (i) *N,N*′-$BidH^+$ ligands: pK_{a1} values of 4.41 and 4.92 for 2,2′-bipyridine and 1,10-phenanthroline, respectively;[36] (ii) *N,O*-BidH: The pK_{a1} value of 5.25 is reported[37,38] for the pK_{a2} of pyridine-2-carboxylic acid and although not accurately known from literature a pK_{a2} values of ca. 4.5 and is estimated for the pyridine-2,4-dicarboxylid acid, based on the corresponding benzene-1,3-dicarboxylate analogue (x = 2, 3, 4);[37−39] (iii) *O,O*′-Bid: the pK_{a1} value of tribromotropolone is estimated to be ∼5, based on the pK_{a1} values of tropolone and the quinoline analogs,[36,40,41] while a pK_{a1} for 3-Hydroxyflavone of 8.35 has been reported.[42] The *N,N*′-$BidH^+$, *N,O*-BidH, and tribromotropolone (*O,O*′-BidH) Bronsted pK_{a1} values vary by about 1 pH unit, while the 3-hydroxyflavone is significantly more basic.

EXPERIMENTAL SECTION

General. All experiments were performed aerobically using double distilled water and methanol. Unless otherwise stated, all chemicals were of reagent grade. $[Re(CO)_5Br]$ was obtained from Strem Chemicals and converted to *fac*-$[ReCO_3Br_3]^{2-}$ according to the method described by Alberto et al.[43] All other chemicals and ligands were purchased from Sigma Aldrich. UV/visible measurements were performed on Varian Cary 50 Conc and Varian 100 UV−visible spectrophotometers with thermostatted automated multicell changers (10 cells virtually simultaneously monitored), equipped with a Julabo F12-mV temperature cell regulator (accurate within 0.1 °C) in 1.000 ± 0.001 cm quartz tandem cuvette cells. The more rapid reactions ($t_{1/2}$ < 20 s) were first evaluated on a third generation Hi Tech SF61DX2 Stopped Flow System equipped with a diode array (dead time <5 ms; 400 nm spectral width scans collected at <5 ms/complete scan), with a thermostatted SHU61DX sample handling unit and an attached Julabu MPV thermostatted water bath (accurate within ±0.05 °C) to select the best absorbance difference regions for the most accurate monitoring of reactions. This was then followed on the stopped-flow in photomultiplier mode (dead time *ca.* 1 ms) to monitor the actual reactions. The values reported (see Supporting Information) consist of the average of 5 individual traces per concentration. The second order rate constants as observed clearly indicate that even the least reactive complexes (**1b** and **2b**) completely solvate to the corresponding methanol species within a few hours, with most requiring only minutes or even seconds. This was confirmed by monitoring the kinetics on freshly prepared solutions, allowing these to stand for different appropriate times, ranging from minutes to hours, and

dx.doi.org/10.1021/ic2013792 | *Inorg. Chem.* 2011, 50, 12486−12498

remonitoring the reactions. No change in the rates of the reactions or deviation from first-order kinetics could be observed, leading to the conclusion that the complexes were completely solvated upon commencement of the kinetic runs to study the substitution processes. Infrared spectra of the complexes were recorded on a Bruker Tensor 27 Standard System spectrophotometer and a Varian Scimitar™ series FT-IR with a laser range of 4000 - 370 cm^{-1} that is coupled to a personal computer. Samples were analyzed as KBr pellets. All ^1H NMR spectra were obtained on Bruker 600 MHz or Varian 300 MHz nuclear magnetic resonance spectrometers at ambient temperature (22 ± 1 °C). When required, solutions were acidified using HNO_3. UV/vis data of products from substitution reactions were obtained assuming complete conversion to the substituted species (as calculated from the corresponding K_1 values determined kinetically). Similarly, IR carbonyl stretching frequencies of these products were obtained as solids in KBr following evaporation of all solvent after completion of the substitution reactions. As stated above, solvation of the aqua complexes proceeded rapidly. Thus, all NMR characterizations of the different aqua species under 'synthesis' actually refer to the deuterated *solvated* species, depending on which solvent was used, and are reported as such. ^1H Chemical shifts were referenced relative to the CH_3OH resonances in methanol-d_4 (3.31 ppm), $CH_3(CO)CH_3$ in acetone-d_6 (2.05 ppm), and $(CH_3)_2SO$) in DMSO-d_6 (2.50 ppm), while ^{13}C NMR spectra were calibrated relative to the ^{13}C resonances for acetone (29.9 ppm), methanol (49.2 ppm), and DMSO (39.5 ppm). The long relaxation times of specifically carbonyl ligands, together with the low solubility of most of the complexes result in many of these not being observed, however, the presence of the carbonyl ligands are clearly detected on the IR spectra.

***fac*-[Re(CO)$_3$(Bipy)(H$_2$O)]NO$_3$·H$_2$O (1).** $[NEt_4]_2[Re(CO)_3Br_3]$ (500 mg, 0.65 mmol) was dissolved in water at pH = 2.2. $AgNO_3$ (330 mg, 2.0 mmol) was added to the solution and stirred for at least eight hours before the precipitate (AgBr) was filtered off (0.374 g, yield = 99.5%, 3 Br eq). 2,2′-Bipyridyl (101.4 mg, 0.7 mmol), dissolved in a small amount of methanol, was added to the filtrate and stirred overnight. A dark-yellow precipitate was filtered off and dried in vacuo. The filtrate was left to crystallize. Dark yellow-red needles, suitable for X-ray diffraction were obtained. Yield = 331 mg (0.631 mmol; 97%). NMR Characterization of ***fac*-[Re(CO)$_3$(Bipy)(CD$_3$SOCD$_3$)]** ^1H NMR (300.13 MHz, CD_3OD) δ 7.61 (t, 2 H, J = 6.5 Hz), 8.11 (t, 2 H, J = 8.2 Hz), 8.34 (d, 2 H, J = 8.2 Hz), 9.01 (d, 2 H, J = 5.6 Hz). $^{13}C\{^1H\}$ NMR (150.96 MHz, CD_3SOCD_3) δ 122.1 (s), 125.4 (s), 138.8 (s), 153.8 (s), 154.0. IR (KBr, cm^{-1}): υ_{CO} = 2008, 1904, 1882. Anal. Calcd: C, 29.77; H, 2.31; N, 8.01. Anal. Found: C, 29.51; H, 2.37; N, 7.99.

***fac*-[Re(CO)$_3$(Phen)(H$_2$O)]NO$_3$.0.5Phen (2).** $[NEt_4]_2[Re(CO)_3Br_3]$ (500 mg, 0.65 mmol) was dissolved in water at pH = 2.2. $AgNO_3$ (330 mg, 2.0 mmol) was added to the solution and stirred for at least eight hours before the precipitate (AgBr) was filtered off. 1,10-phenantroline (128.7 mg, 0.7 mmol) dissolved in a small amount of methanol was added to this. The mixture was left to stir overnight. Dark yellow cuboid crystals were obtained after filtration and used for X-ray diffraction analysis. Yield = 165 mg (0.267 mmol; 41%). NMR Characterization of ***fac*-[Re(CO)$_3$(Phen)(CD$_3$OD)]** ^1H NMR (300.13 MHz, CD_3OD) δ 8.03 (dd, 2 H, J = 8.2 − 5.2), 8.21 (s, 2 H), 8.80 (d, 2 H, J = 8.4 Hz), 9.51 (d, 2 H, J = 5.1 Hz). $^{13}C\{^1H\}$ NMR (150.94 MHz CD_3OD) δ 113.4, 126.8, 127.9, 139.4, 142.9, 144.1. IR (KBr, cm^{-1}): υ_{CO} = 2008, 1932, 1908. Anal. Calcd.: C, 40.65; H, 2.27; N, 9.03. Anal. Found: C, 41.02; H, 2.54, N, 8.89.

[NEt$_4$][Re(CO)$_3$(2,4-dPicoH)Br] (3). $[NEt_4]_2[Re(CO)_3Br_3]$ (300 mg, 0.389 mmol) was dissolved in 30 mL methanol. 2,4-Pyridinedicarboxylic acid (65.1 mg, 0.390 mmol) was added to the mixture as a solid and stirred at 50 °C for 17 h. The product precipitated from the reaction mixture after a few days. This compound was also obtained by adding NaBr (1:1) to solutions of **4** and allowing to stand for a few days in a methanol solution. Yield = 148.3 mg (0.229 mmol; 59%). ^1H NMR (300.13 MHz, CD_3COCD_3) δ 1.38 (t, 12H (NEt_4), J = 1.8 Hz, 7.2 Hz), 3.51 (q, 8H (NEt_4), J = 7.2 Hz), 8.21 (dd, 1H, J = 2.4 Hz, 6.0 Hz), 8.54 (d, 1H, J = 1.2 Hz), 9.03 (d, 1H, J = 6H z). $^{13}C\{^1H\}$ NMR (150.94 MHz, CD_3COCD_3) δ 7.38, 53.0, 127.2, 129.2, 143.8, 154.4, 165.0, 165.8. IR (KBr, cm^{-1}): υ_{CO} = 2020, 1893. Anal. Calcd.: C, 33.44; H, 3.74; N, 4.33. Anal. Found: C, 34.00; H, 3.82; N, 4.05.

***fac*-[Re(CO)$_3$(2,4-dPicoH)(H$_2$O)] (4).** $[NEt_4]_2[Re(CO)_3Br_3]$ (300 mg, 0.389 mmol) was stirred in 40 mL of water at pH 2.2 for ∼20 min until dissolved. $AgNO_3$ (198 mg, 1.17 mmol) was added to the solution and stirred for 24 h at room temperature. The precipitate, AgBr, was filtered off and weighed (220 mg). 2,4-Pyridinedicarboxylic acid (65 mg, 0.389 mmol) was added to the filtrate as a solid and stirred for 36 h. The solution turned bright yellow with a light yellow precipitate. The product was filtered off, dried and weighed. Crystals were obtained by slow evaporation of the filtrate. Yield = 140 mg (0.308 mmol; 79%). NMR Characterization of ***fac*-[Re(CO)$_3$(2,4-dPicH)(CD$_3$OD)]** ^1H NMR (300.13 MHz, CD_3COCD_3) δ 8.06 (d, 1H, J = 1.2 Hz), 8.44 (dd, 1H, J = 1.2 Hz, 5.4 Hz), 9.48 (d, 1H, J = 6.0 Hz). $^{13}C\{^1H\}$ NMR (150.94 MHz, CD_3OD) δ 126.0, 128.1, 142.7, 151.1, 153.0, 164.4, 173.3, 192.8, 195.9, 196.0. IR (KBr, cm^{-1}): υ_{CO} = 2035, 1919. Anal. Calcd.: C, 26.43; H, 1.33; N, 3.0. Anal. Found: C, 26.40; H, 1.88; N, 2.77.

***fac*-[Re(CO)$_3$(2,4-dQuinH)(H$_2$O)] (5).** $[NEt_4]_2[Re(CO)_3Br_3]$ (300 mg, 0.389 mmol) was stirred in 40 mL of water at pH 2.2 for ∼20 min until dissolved. $AgNO_3$ (198 mg, 1.17 mmol) was added to the solution and stirred for 24 h at room temperature. The precipitate, AgBr, was filtered off and weighed (222 mg). 2,4-Quinolinedicarboxylic acid (84.5 mg, 0.389 mmol) was added to the solution as a solid, stirred for 24 h at 85 °C. The solution turned yellow/orange and the product precipitated out as orange plate-like crystals. Yield = 174 mg (0.345 mmol; 89%). NMR Characterization of ***fac*-[Re(CO)$_3$(2,4-dQuinH)(CD$_3$OD)]** ^1H NMR (300.13 MHz, CD_3COCD_3) δ 7.81 (s, 1H), 8.07 (t, 1H, J = 9.0 Hz), 8.30 (t, 1H, J = 9.0 Hz), 8.92 (d, 1H, J = 9.0 Hz), 9.08 (d, 1H, J = 9.0 Hz). $^{13}C\{^1H\}$ NMR (150.94 MHz, CD_3OD) δ 122.8, 126.9, 127.2, 127.5, 128.8, 130.4, 132.6, 147.3, 152.3. IR (KBr, cm^{-1}): υ_{CO} = 2034, 1936, 1886. Anal. Calcd: C, 32.19; H, 2.39; N, 2.68. Anal. Found: C, 32.80; H, 2.12; N, 2.40.

***fac*-[Re(CO)$_3$(2,4-dQuinH)Py] (6).** *fac*-$[Re(CO)_3(2,4\text{-dQuinH})(H_2O)]$ (**5**) (20 mg, 0.04 mmol) was dissolved in methanol. Pyridine (3.2 mg, 0.04 mmol) in 2 mL of methanol was slowly added to the stirring solution and left to stir for 10 h at 35 °C. The orange solution was left in the fridge for a few days and yellow needles were collected. Yield =18 mg (0.032 mmol; 79%). ^1H NMR (300.13 MHz, CD_3COCD_3) δ 7.47 (t, 2H (Py), J = 7.2 Hz), 7.97 (t, 1H, J = 8.4 Hz), 8.07 (t, 1H, J = 7.8 Hz), 8.31 (tt, 1H (Py), J = 1.2 Hz, 9.0 Hz), 8.45 (dd, 2H (Py), J = 6.6 Hz, 12 Hz), 8.54 (s, 1H), 8.97 (d, 1H, J = 9.0 Hz), 9.00 (d, 1H, J = 8.4 Hz). $^{13}C\{^1H\}$ NMR (150.94 MHz, CD_3OD) δ 123.0, 123.8, 126.2, 128.6, 129.4, 129.7, 131.1, 137.9, 142.4, 146.4, 150.0, 150.3, 160.6. IR (KBr, cm^{-1}): υ_{CO} = 2024, 1926, 1869. Anal. Calcd: C, 44.72; H, 2.50; N, 6.52. Anal. Found: C, 44.60; H, 2.34; N, 5.86.

***fac*-[Re(CO)$_3$(TropBr$_3$)(H$_2$O)] (7).** Prepared as reported in literature and characterized accordingly.[44]

***fac*-[Re(CO)$_3$(Flav)(H$_2$O)] (8).** $[NEt_4]_2[Re(CO)_3Br_3]$ (500 mg, 0.649 mmol) was stirred in 40 mL of water at pH 2.2 for ∼20 min until dissolved. $AgNO_3$ (330 mg, 1.95 mmol) was added to the solution and stirred for 24 h at room temperature. The precipitate, AgBr, was filtered off and weighed. 3-Hydroxyflavone (183 mg, 0.768 mmol) was added to the solution as a solid. It was refluxed for 24 h at 90 °C. With time, the solution turned yellow and a bright yellow precipitate formed. The mixture was cooled down and filtrated. The filtrate was left to stand. It was not possible to obtain good quality single crystals for X-ray diffraction experiments and it was recrystallized from methanol instead (see below). Yield: 314 mg (0.598 mmol, 92%). NMR characterization of ***fac*-[Re(CO)$_3$(Flav)(CD$_3$OD)]** ^1H NMR (300.13 MHz, CD_3COCD_3) δ 7.48 (d, 1H, J = 0.6 Hz), 7.51 (dd, 2H, J = 7.2 Hz, 15.6 Hz), 7.59 (t, 1H, J = 7.8 Hz), 7.77 (d, 1H, J = 8.4 Hz), 7.83 (td, 1H, J = 1.2 Hz, 7.8 Hz), 8.18 (dd, 1H, J = 1.8 Hz, 8.4 Hz), 8.32 (d, 2H, J = 7.8 Hz). $^{13}C\{^1H\}$ NMR (150.94 MHz, C_3D_6O) δ 118.3, 118.4, 121.1, 123.8, 124.4, 125.0, 127.5, 127.6, 128.5, 128.6, 129.9, 133.6, 138.7, 155.4, 173.0, 197.9, 198.3, 198.8. IR (KBr, cm^{-1}): υ_{CO} = 2013, 1885. Anal. Calcd: C, 41.14; H, 2.11. Anal. Found: C, 42.01; H, 2.23.

dx.doi.org/10.1021/ic2013792 | Inorg. Chem. 2011, 50, 12486–12498

Table 1. Crystal Data for *fac*-[Re(CO)$_3$(Phen)(H$_2$O)]·NO$_3$·0.5Phen (**2**), *fac*-[Re(CO)$_3$(2,4-dQuinH)(H$_2$O)] (**5**), *fac*-[Re(CO)$_3$(2,4-dQuinH)Py] (**6**), and *fac*-[Re(CO)$_3$(Flav)(CH$_3$OH)]·CH$_3$OH (**9**)

	2	**5**	**6**	**9**
formula	$C_{21}H_{14}N_4O_7Re$	$C_{14}H_8NO_9Re$	$C_{24}H_{16}N_3O_7Re$	$C_{20}H_{17}O_8Re$
fw (g·mol^{-1})	620.57	520.42	644.61	571.54
cryst syst	monoclinic	monoclinic	triclinic	triclinic
space group	$P2/n$ (13)	$P2_1/c$ (14)	(2)	(2)
a (Å)	10.917(5)	14.843(5)	6.386(5)	7.551(5)
b (Å)	11.269(5)	13.975(5)	9.318(5)	9.768(5)
c (Å)	17.271(5)	7.460(5)	19.509(5)	13.373(5)
α (deg)	90.000(5)	90.000(5)	103.592(5)	94.173(5)
β (deg)	90.675(5)	100.701(5)	93.747(5)	95.504(5)
γ (deg)	90.000(5)	90.000(5)	95.850(5)	102.569(5)
V (Å^3)	2124.6(15)	1520.5(13)	1117.7(11)	953.8(9)
Z	4	4	2	2
D_{calcd} (mg·m^{-3})	1.940	2.273	1.901	1.990
μ (mm^{-1})	5.772	8.044	5.474	6.416
T (K)	295	100	100	273
λ (Å)	0.71069	0.71073	0.71073	0.71073
cryst size (mm)	0.21 × 0.14 × 0.09	0.25 × 0.219 × 0.06	0.266 × 0.158 × 0.142	0.361 × 0.232 × 0.024
F(000)	1196	984	624	552
R_{int}	0.0472	0.0514	0.0381	0.0476
GOF	0.971	1.026	1.107	1.061
R_1 [$I > 2\sigma(I)$]	0.0335	0.0342	0.0293	0.0285
R_1 (all data)	0.0574	0.0486	0.0321	0.0356

***fac*-[Re(CO)$_3$(Flav)(CH$_3$OH)]·CH$_3$OH (9).** This was obtained by dissolving 20 mg (0.038 mmol) of the yellow *fac*-[Re(CO)$_3$(Flav)(H$_2$O)] precipitate in methanol. Small yellow crystals, suitable for single crystal X-ray diffraction experiments were collected after ∼21 days. Yield: 16 mg (0.028 mmol, 74%). NMR Characterization of ***fac*-[Re(CO)$_3$(Flav)(CD$_3$COCD$_3$)]** ^{1}H NMR (300.13 MHz, CD$_3$COCD$_3$) δ 3.31 (s, 3H), 7.48 (dd, 2H, 7.2 Hz, J = 15.0 Hz), 7.5 (d, 1H, J = 0.6 Hz), 7.52 (t, 1H, J = 7.8 Hz), 7.82 (t, 1H, J = 7.2 Hz), 7.82 (d, 1H, J = 8.4 Hz), 8.19 (d, 1H, J = 7.2 Hz), 8.25 (d, 2H, J = 7.8 Hz). ^{13}C{^{1}H} NMR (150.94 MHz, CD$_3$OD) δ 117.5, 121.0, 125.1, 127.4, 127.6, 127.7 128.2, 128.4, 129.1, 129.9, 133.6, 137.4, 138.7, 151.5. IR (KBr, cm^{-1}): υ_{CO} = 2015, 1892. Anal. Calcd: C, 42.18; H, 2.65. Anal. Found: C, 42.02, H, 2.49.

***fac*-[Re(CO)$_3$(Pico)(H$_2$O)]·H$_2$O (10) and *fac*-[Re(CO)$_3$(Quin)(H$_2$O)]·H$_2$O (11).** Prepared as reported in literature and characterized accordingly.[45,46]

***fac*-[Re(CO)$_3$(Bipy)Br] (12).** [NEt$_4$]$_2$[Re(CO)$_3$(Br)$_3$] (300 mg, 0.389 mmol) was dissolved in 30 mL of methanol. 2,2′-Bipyridine (56.4 mg, 0.389 mmol), dissolved in a small amount of methanol, was added to the filtrate and stirred overnight at 50 °C. A dark-yellow solution formed and was left to crystallize. Yield =158 mg (0.312 mmol; 80%). ^{1}H NMR (CD$_3$SOCD$_3$): δ 7.14 (t, 2 H, J = 6.5 Hz), 7.70 (t, 2 H, J = 8.2 Hz), 8.59 (d, 2 H, J = 5.6 Hz), 8.93 (d, 2 H, J = 8.2 Hz). ^{13}C{^{1}H} NMR (CD$_3$SOCD$_3$) δ 110.3, 123.7, 146.7, 153.7, 158.3. Anal. Calcd: C, 30.84; H, 1.59; N, 5.53. Anal. Found: C, 30.43; H, 1.62; N, 5.61.

***fac*-[Re(CO)$_3$(Phen)Br] (13).** [NEt$_4$]$_2$[Re(CO)$_3$(Br)$_3$] (300 mg, 0.389 mmol) was dissolved in 30 mL methanol and 1,10-Phenantroline (71.52 mg, 0.389 mmol) was added to this. The mixture was heated to 50 °C and left to stir overnight. A yellow solution formed and was left to crystallize. Yield = 156 mg (0.294 mmol; 76%). ^{1}H NMR (CD$_3$OD) δ 7.58 (t, 2 H, 5.2 Hz), 7.93 (s, 2H), 8.38 (d, 2 H, 8.2 Hz), 8.82 (d, 2 H, J = 5.1 Hz). ^{13}C{^{1}H} NMR (CD$_3$OD) δ 112.1, 126.7, 129.8, 139.6, 147.8, 150.6. Anal. Calcd: C, 34.03; H, 1.33; N, 5.29. Anal. Found: C, 34.22; H, 1.29; N, 5.43.

X-ray Structure Determinations. Diffraction data for **2**, **5**, **6**, and **9** were collected at different temperatures as indicated in Table 1 on either a Bruker SMART CCD 1K (**2**) or Bruker X8 ApexII 4K (**5**, **6**, and **9**) diffractometers using monochromated Mo Kα radiation. Cell parameters were refined by using the program SAINT-Plus.[47] SADABS[48] was used for absorption corrections. The structures were solved by direct methods and refined on F^2 using anisotropic displacement parameters for all non-H atoms. Structure solutions and refinements were performed with the SHELXL-97[49,50] and WinGX[51] respectively, while molecular graphics were done with DIAMOND.[52] Aromatic hydrogen atoms were placed in geometrically idealized positions (C−H = 0.93 Å) and constrained to ride on their parent atoms with U_{iso}(H) = 1.2U_{eq}(C). Aqua hydrogen atoms were located from Fourier difference maps and constrained with equal O−H distances. The Br atom and the *trans*-CO ligand in fac-[Re(CO)$_3$(Bipy)(Br)] (**12**) crystallized with a 50% statistical disorder and is reported separately in the Supporting Information.

Equilibrium Studies. The substitution of MeOH in the *fac*-[Re(CO)$_3$(*L*,*L*′-Bid)(MeOH)]^n complexes by a range of entering ligands could be studied as pseudo first-order processes defined by the simple equilibrium which exists, as indicated in eq 1.

$$[Re(CO)_3(L,\ L'\text{-Bid})(CH_3OH)]^- + X \underset{k_{-1}}{\overset{k_1,K_1}{\rightleftharpoons}} [Re(CO)_3(L,\ L'\text{-Bid})X]^n + CH_3OH \quad (1)$$

$n = (1 + m)$; $m = 0, -1$ = charge of chelated bidentate ligand, while the charge of the entering nucleophile X is not specified.

The stability constant (denoted by K_1) for the reaction between the *fac*-[Re(CO)$_3$(*L*,*L*′-Bid)(MeOH)]^n complex and monodentate entering ligands (indicated X) has been determined kinetically using the definition $K_1 = k_1/k_{-1}$, see below. Alternatively, it was obtained by nonlinear least-squares analysis using the established relationship based on UV/vis data, $A_{obs} = (A_M + A_{ML}K_1[X])/(1 + K_1[X])$, as reported previously,[39] derived from Beer's law, mass balance and the definition of K_1 for the overall reaction, where A_M and A_{ML} represent the absorbance of the *fac*-[Re(CO)$_3$(*L*,*L*′-Bid)(MeOH)]^n and *fac*-[Re(CO)$_3$(*L*,*L*′-Bid)(X)]^n complexes, A_{obs} the observed absorbance and [X] the concentration of the entering ligand, respectively.[25,25] Only one reaction was observed spectroscopically during this study, indicating a one-step process for all the different entering nucleophiles X investigated.

Kinetic Data Treatment. All the kinetic runs were performed under pseudo-first-order conditions with the ligand in large excess in each case. Least-squares analyses were performed on the absorbance vs

dx.doi.org/10.1021/ic2013792 | Inorg. Chem. 2011, 50, 12486−12498

Table 2. Selected Bond Distances (Å) and Angles (deg) for 2, 5, 6, and 9[a]

	2	5	6	9
Re−N1	2.168(4)	2.220(5)	2.247(3)	
Re−N2/O5	2.174(4)			2.141(3)
Re−O4		2.145(4)	2.117(3)	2.147(3)
Re−C1	1.914(6)	1.908(7)	1.905(4)	1.905(5)
Re−C2	1.929(6)	1.902(6)	1.907(5)	1.906(5)
Re−C3	1.893(6)	1.910(6)	1.919(5)	1.893(5)
Re−X	2.162(3) − O4	2.182(4) − O6	2.203(4) − N2	2.204(4) − O7
L−Re−L′	75.86(15)[b]	75.25(15)[c]	75.67(13)[c]	76.24(11)[d]
L−L′	2.669(5)[e]	2.665(6)[f]	2.678(5)[f]	2.647(4)[g]
C1−Re−C2	90.2(3)	85.8(2)	87.13(18)	88.61(19)
C3−Re−X	174.96(18)−O4	174.5(2)−O6	178.03(16)−N2	173.89(16)−O7
C3−Re−C1	87.2(2)	89.6(3)	88.86(19)	90.1(2)
C3−Re−C2	89.9(2)	88.5(2)	89.82(19)	85.7(2)
C3−Re−N1	96.05(18)	94.3(2)	94.41(16)	
C3−Re−N2	96.16(19)			
C3−Re−O4		97.77(19)	97.25(17)	92.36(17)
C3−Re−O5				100.77(17)
Re−C1−O1	175.1(5)	177.9(6)	177.3(4)	178.3(4)
Re−C2−O2	178.9(6)	178.1(6)	177.8(4)	178.3(4)
Re−C3−O3	178.3(5)	178.6(5)	179.1(4)	176.8(4)

[a]X = py, H_2O, or MeOH. [b]N1−Re−N2. [c]N1−Re−O4. [d]O5−Re−O4. [e]N1−N2. [f]N1−O4. [g]O4−O5.

time data obtained from the kinetics runs to appropriate functions using MicroMath Scientist.[53] The solid lines in the figures represent computer least-squares fits of data, while experimental values are represented as individual points, denoted by selected symbols. The concentration dependence of the pseudo-first-order rate constant (k_{obs}) for the substitution process of the aqua ligand in the *fac*-[$Re(CO)_3$(*L*,*L*′-Bid)(MeOH)]^n complexes by monodentate entering ligands (indicated X) is given by eq 2,[25,39] monitoring of the kinetics at conditions where [X] ≫ [Re], with typical metal concentrations ranging from 4×10^{-5} to 1×10^{-4} M. The rates and concentration dependences obtained in this study assumes that the aqua complexes, immediately upon dissolution in methanol, exchange the coordinated aqua to form the corresponding *fac*-[$Re(CO)_3$(*L*,*L*′-Bid)(MeOH)]^n complexes. The corresponding methanol solvolysis reactants are thus indicated throughout by using "b" as suffix, that is, **1b**, **2b**, etc. Actvation parameters were determined from Eyring plots, including the use of global fitting techniques.

$$k_{obs} = k_1[X] + k_{-1} \quad (2)$$

RESULTS

Synthesis. Special care had to be taken for the synthesis of the aqua complexes *fac*-[$Re(CO)_3$(*L*,*L*′-Bid)(H_2O)]^n **1a**, **2a**, **4a**, **5a**, **7a**, **8a**, **10a**, and **11a**, to ensure that the triaqua species were formed before addition of the bidentate ligand. All the aqua compounds were synthesized by first subjecting [$Re(CO)_3Br_3]^{2-}$ to halide abstraction using three equivalents of $AgNO_3$ and stirring at room temperature for 12−24 h. The AgBr precipitate was dried and weighed (as reported for *fac*-[$Re(CO)_3$(Bipy)(H_2O)]NO_3·H_2O (**1**)) to ensure quantitative replacement of all three Br^- ligands by H_2O molecules. The pH of the solution, when preparing the aqua complexes, was adjusted to ∼2.2 every time to minimize potential dimer formation due to hydroxo complexes. The ^1H and ^{13}C NMR and elemental analysis results support the synthetic results.

X-ray Crystallography. The X-ray crystal structures for **2**, **5**, **6**, and **9** were determined and crystallographic data, selected bond angles and bond lengths are reported in Tables 1 and 2. The complex structures of **2**, **5**, **6**, and **9** are shown in Figure 1a−d, respectively, with their corresponding atom numbering schemes. The bonding distances of Re to the monodentate ligands (other than CO) are indicated in Table 2 by Re−X.

Spectroscopic Characterization of *fac*-[$Re(CO)_3$(*L*,*L*′-Bid)(X)] Complexes. More than twenty respective reactants and products from ligand substitution reactions of the coordinated methanol in the *fac*-[$Re(CO)_3$(*L*,*L*′-Bid)-(MeOH)]^n complexes were characterized in situ by UV−vis, and the data are reported in Table 3. The rates and concentration dependences obtained in this study assumes that the aqua complexes, immediately upon dissolution in methanol, exchanges the coordinated aqua to form the corresponding solvated *fac*-[$Re(CO)_3$(*L*,*L*′-Bid)(MeOH)]^n complexes. The products were also confirmed by the kinetic runs, where simple first-order substitution processes were observed for all the reactions studied, clearly yielding only one product. All these product complexes were defined by typical UV−vis spectra indicative of the mono substitution which has been affected. Moreover, IR data for some twenty of the reactants and products are additionally reported which have been obtained from KBr pellets.

Thermodynamic Equilibrium Studies. The substitution of the coordinated methanol in the *fac*-[$Re(CO)_3$(*L*,*L*′-Bid)(MeOH)]^n complexes by a range of entering nucleophiles could be studied as pseudo-first-order processes defined by the simple equilibrium, which exists as indicated in eq 1. As outlined above, the rates and concentration dependences obtained in this study assumes that the aqua complexes, immediately upon dissolution in methanol, exchanges the coordinated aqua to form the corresponding *fac*-[$Re(CO)_3$(*L*,*L*′-Bid)(MeOH)]^n complexes. Further confirmation to this effect stems from the isolation and characterization, also by X-ray structural studies, of complexes wherein methanol is coordinated in the aqua site, as manifested by **9** as described here as well as those recently reported.[54] The stability constants have been calculated as described above and are reported in Tables 4 and 5. Figure 2 illustrates the data treatment to determine the stability constants thermodynamically.

dx.doi.org/10.1021/ic2013792 | *Inorg. Chem.* 2011, 50, 12486−12498

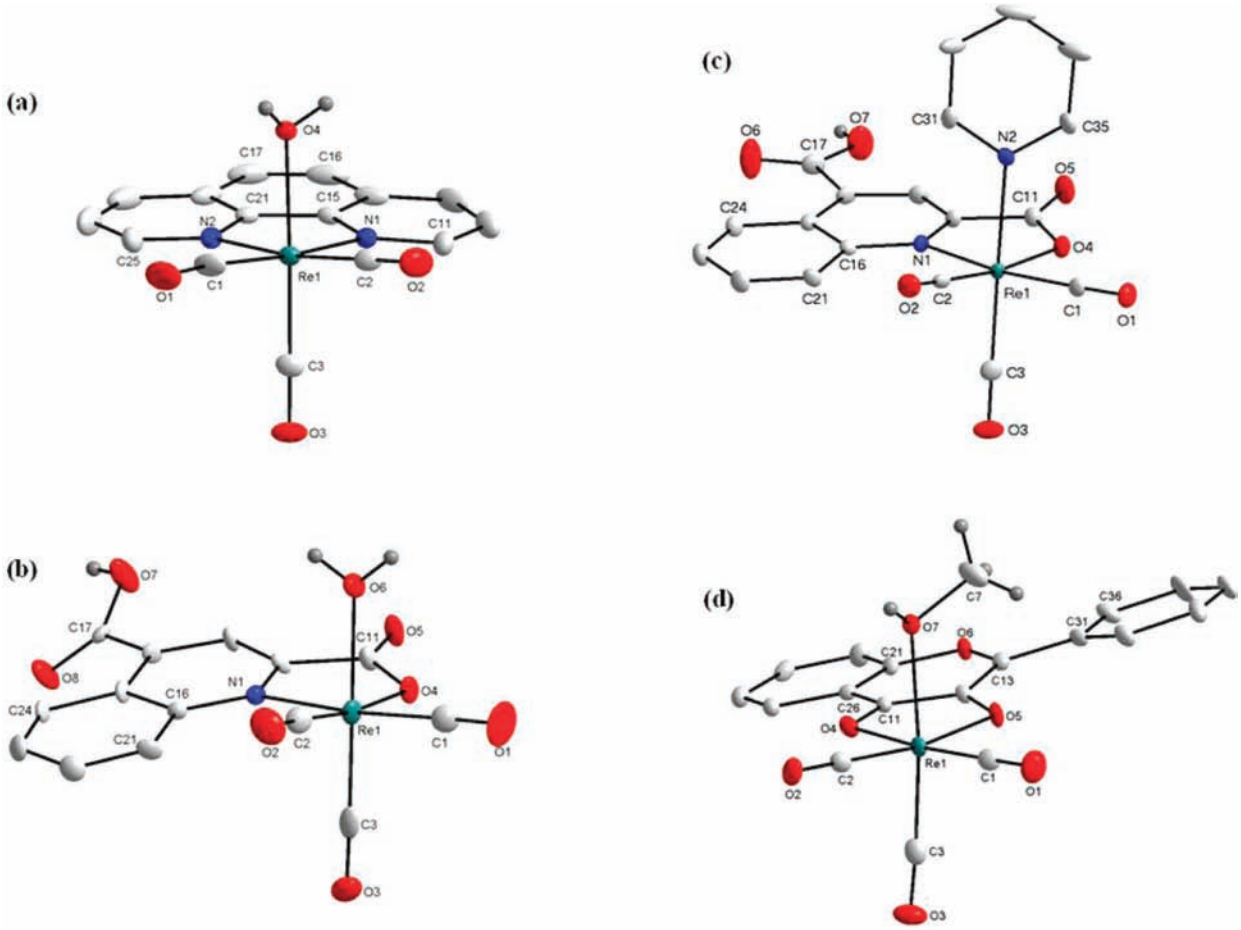

Figure 1. Molecular structures of the rhenium complexes (a) **2a** in *fac*-[$Re(CO)_3(Phen)(H_2O)]NO_3$·0.5Phen (**2**), (b) **5a** in *fac*-[$Re(CO)_3$(2,4-dQuinH)$(H_2O)]$·H_2O (**5**), (c) **6a** in *fac*-[$Re(CO)_3$(2,4-dQuinH) Py]Py (**6**), and (d) **9a** in *fac*-[$Re(CO)_3(Flav)(CH_3OH)]$.CH_3OH (**9**) [only complexes indicated, H-atoms (except for the oxygen protons) and solvate molecules are omitted for clarity].

Table 3. Spectroscopic Data for *fac*-[$Re(CO)_3$(*L*,*L*′-Bid)(X)]^n Complexes[a]

compound	λ_{max} (nm)	ε (M^{-1} cm^{-1})	$\nu_{(C\equiv O)}$ (KBr; cm^{-1})		
$[Re(CO)_3(Bipy)(H_2O)]^+$, **1a**[b]	350[b]	3333	2008	1904	1882
$[Re(CO)_3(Phen)(H_2O)]^+$, **2a**[b,c]	360	2909	2008	1932	1908
$[Re(CO)_3(Pico)(H_2O)]$, **10a**[b]	313	5140	2022	1908	1874
$[Re(CO)_3$(2,4-dPicoH)$(H_2O)]$, **4a**[b]	339	4280	2035	1919	
$[Re(CO)_3$(2,4-dPicoH)$(Br)]^-$, **3a**	343	3620	2021	1893	
$[Re(CO)_3$(2,4-dPicoH)(Py)]	315	5550	2030	1929	1908
$[Re(CO)_3$(2,4-dPicoH)(Pz)]	327	4460	2034	1899	
$[Re(CO)_3$(2,4-dPicoH)(Im)]	313	5300	2030	1926	1906
$[Re(CO)_3$(2,4-dPicoH)(DMAP)]	342	3220	2018	1883	
$[Re(CO)_3(Quin)(H_2O)]$, **11a**[b,d]	320	5800	2018	1920	1880
$[Re(CO)_3$(2,4-dQuinH)$(H_2O)]$, **5a** [b]	352	51900	2034	1936	1886
$[Re(CO)_3$(2,4-dQuinH)$(Br)]^-$	328	49500	2020	1904	1870
$[Re(CO)_3$(2,4-dQuinH)(Py)], **6a**	358	49900	2024	1926	1869
$[Re(CO)_3$(2,4-dQuinH)(DMAP)]	371	29000	2017	1878	
$[Re(CO)_3(TropBr_3)(H_2O)]$, **7a** [b]	357	12880	2024	1886	
$[Re(CO)_3(TropBr_3)(Br)]^-$	372	10500	2008	1900	1876
$[Re(CO)_3(TropBr_3)(Py)]$	356	12480	2015	1904	1869
$[Re(CO)_3(TropBr_3)(DMAP)]$	356	12200	2017	1893	
$[Re(CO)_3(Flav)(H_2O)]$, **8a** [b]	343	26500	2013	1885	
$[Re(CO)_3(Flav)(Br)]^-$	342	25000	1999	1863	
$[Re(CO)_3(Flav)(CH_3OH)]$, **9a**	343	26600	2015	1892	
$[Re(CO)_3(Flav)(Py)]$	342	25480	2012	1897	1860
$[Re(CO)_3(Flav)(DMAP)]$	344	15450	2006	1908	1888

[a]X = monodentate ligands as indicated. [b]Isolated complexes indicated; solvolysis to form the corresponding MeOH species upon dissolution in methanol. [c]Additional bands: λ_{max} (nm); ε (M^{-1} cm^{-1}); High energy band 223, 4218. [d]Low energy band 350, 4200.

dx.doi.org/10.1021/ic2013792 | *Inorg. Chem.* 2011, 50, 12486–12498

Table 4. Rate and Equilibrium Constants for the Reactions of *N,N*-Bidentate Ligand Rhenium(I) Complexes *fac*-[Re(CO)$_3$(Bipy)(MeOH)]$^+$ (1b) [a] and *fac*-[Re(CO)$_3$(Phen)(MeOH)]$^+$ (2b) [a] with Different Entering Ligands in Methanol at 25.0 °C

	1b			2b		
	10^3 k_1 ($M^{-1}s^{-1}$)	10^3 k_{-1} (s^{-1})	K_1 [b] (M^{-1})	10^3 k_1 ($M^{-1}s^{-1}$)	10^3 k_{-1} (s^{-1})	K_1 [b] (M^{-1})
Cl^-	17(2)	0.16(1)	100(11)	36(4)	0.41(3)	87(11)
Br^-	42(7)	0.65(2)	60(8)	50(3)	0.59(3)	84(7)
I^-	49(3)	0.68(1)	70(5)	53(1)	0.7(1)	76(11)
Py	0.096(1)	0.0012(1)	8.0(7)	0.064(3)	0.0058(4)	11(1)
m-Mepy	0.025(1)	0.008(1)	3.0(4)	0.012(1)	0.005(2)	2.4(9)
p-Mepy	0.028(1)	0.0047(1)	5.0(2)	0.014(1)	0.0035(1)	4.0(3)
PTA	12.3(1)	0.12(2)	100(20)	7.9(1)	0.11(1)	70(9)
Metu	17.3(1)	0.011(1)	157(14)	13.7(1)	0.11(1)	120(11)

[a] The coordinated methanol substitution in **1b** and **2b**; where **b** suffix indicates the corresponding methanol coordinated rhenium(I) complex of **1** and **2**, respectively. [b] $K_1 = k_1/k_{-1}$; eq 1

Table 5. Rate Constants and Equilibrium Constants for the Reactions of *N,O*- and *O,O′*-Bidentate Ligand Rhenium(I) Complexes: [a] *fac*-[Re(CO)$_3$(2,4-dPicoH)(MeOH)] (4b) and *fac*-[Re(CO)$_3$(2,4-dQuinH)(MeOH)] (5b), *fac*-[Re(CO)$_3$(Pico)(MeOH)] (10b), *fac*-[Re(CO)$_3$(Quin)(MeOH)] (11a), *fac*-[Re(CO)$_3$(TropBr$_3$)(MeOH)] (7b) and *fac*-[Re(CO)$_3$(Flav)(MeOH)] (9a) with Different Entering Ligands in Methanol at 25.0 °C

	10^3 k_1 ($M^{-1}s^{-1}$)	10^3 k_{-1} (s^{-1})	K_1 [b] (M^{-1})	10^3 k_1 ($M^{-1}s^{-1}$)	10^3 k_{-1} (s^{-1})	K_1 [b] (M^{-1})
	[Re(CO)$_3$(2,4-dPicoH)(MeOH)] **4b**			[Re(CO)$_3$(2,4-dQuinH)(MeOH)] **5b**		
Br^-	15.7(2)	0.63(8)	25(3)			
Py	1.641(8)	0.030(2)	21(1)	3.31(2)	0.051(7)	65(9) [c]
DMAP	3.21(4)	0.11(1)	29(3)	6.52(9)	0.025(3)	260(30) [d]
Pz	2.336(9)	0.016(3)	146(27)			
Im	1.44(4)	0.070(5)	21(2)			
	[Re(CO)$_3$(Pico)(MeOH)] **10b**			[Re(CO)$_3$(Quin)(MeOH)] **11b**		
Br^-	11.8(1)	0.8(1)	15(2)	29.6(3)	0.7(1)	42(6)
I^-	14(1)	0.64(1)	22(2)	28.0(1)	0.9(1)	31(4)
Py	1.6(1)	0.0084(1)	190(10)	3.9(1)	0.02(1)	195(97)
	[Re(CO)$_3$(TropBr$_3$)(MeOH)] **7b**			[Re(CO)$_3$(Flav)(MeOH)] **9a**		
Br^-	70.6(4)	4(1)	18(4)	$7.2(3) \times 10^3$	$3.17(9) \times 10^3$	2.5(2)
Py	20.3(7)	1.6(2)	12(2) [e]	$1.38(8) \times 10^3$	0.3(1)	$4.6(1) \times 10^3$
DMAP	34.5(7)	0.26(2)	133(11) [f]	$5.1(2) \times 10^3$	0.16(4)	$3.2(8) \times 10^4$

[a] The coordinated methanol substitution in **4b** and **5b**, **10b** and **11b** (*N,O*-Bid), and **7b** and **8b** (O,O′-Bid) (**b** suffix indicates the corresponding coordinated methanol rhenium(I) complexes of **4**, **5**, **7**, **8**, **10**, and **11**, respectively. [b] $K_1 = k_1/k_{-1}$; eq 1. [c] K_1 = 17(4) M^{-1} from abs vs [py] data. [d] K_1 = 47(9) M^{-1} from abs vs [DMAP] data. [e] K_1 = 5(1) M^{-1} from abs vs [py] data. [f] K_1 = 31(7) M^{-1} from abs vs [DMAP] data, Figure 2.

Kinetics of Coordinated Methanol Substitution. The substitution kinetics of MeOH in the *fac*-[Re(CO)$_3$(*L,L′*-Bid)(MeOH)]^n complexes by various entering ligands could be studied as simple first-order processes defined by a single equilibrium, as described by eq 1.

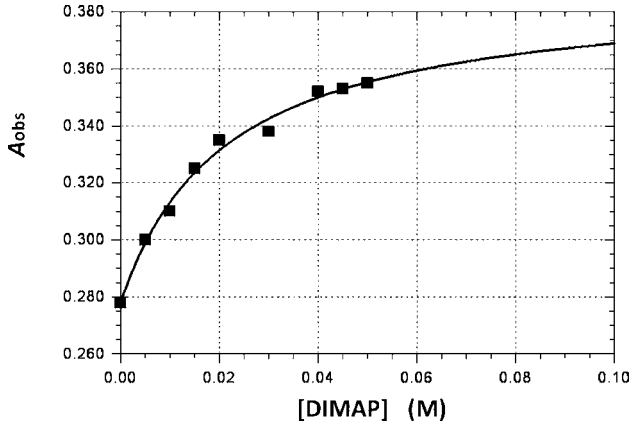

Figure 2. Determination of the stability constant K_1 for the coordinated methanol substitution reaction of *fac*-[Re(CO)$_3$(2,4-dQuinH)(MeOH)] by DMAP from typical UV–vis spectral change observed vs. [DMAP]. [Re] = 1.0×10^{-4} M, 25.0 °C, in methanol.

Previous studies indicated that the substitution of H_2O in *fac*-[Re(CO)$_3$(H$_2$O)$_3$]$^+$ by different ligands proceeded by simple steps to yield predominantly mono-, di, or trisubstituted products.[6,32,33] The identity of the monosubstitution products in this study were confirmed by chemical and spectroscopic analysis, and by X-ray structures, as for example, reported for **6** as well as previously published structure reports.[55,56] To further ensure that the reactions that were observed were not the liberation of the bidentate ligand, solutions of *fac*-[Re(CO)$_3$(*L,L′*-Bid)(H$_2$O)]^n and different entering ligands were evaluated by ^{1}H NMR and IR spectroscopy. No tendency of bidentate ligand dissociation could be observed, nor changes in the absorbance spectra.

Because of the poor solubility of all these complexes in water, the reactions were performed in methanol, thus inducing the formation of the corresponding methanol solvated complexes. The stability of all the complexes in methanol was established by monitoring solutions over several days on a UV–vis

dx.doi.org/10.1021/ic2013792 | Inorg. Chem. 2011, 50, 12486–12498

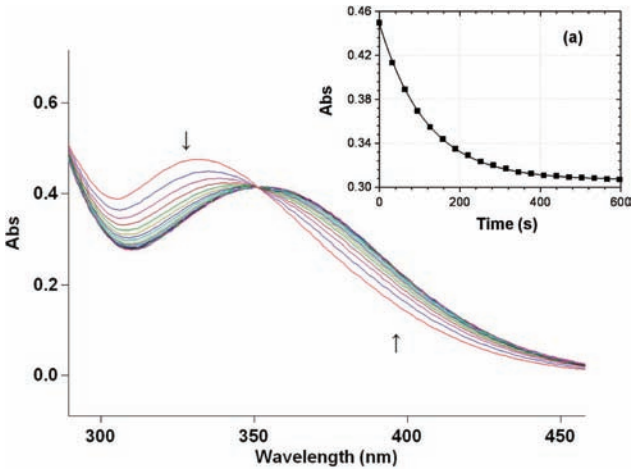

Figure 3. Typical UV–vis spectral change for the coordinated methanol substitution reaction of *fac*-$[Re(CO)_3(2,4\text{-dPicoH})(MeOH)]$ with Br^--ions; [Re] = 1.0×10^{-4} M, $[Br^-]$ = 0.5 M, 25.0 °C, Δt = 30 s, t_{tot} = 800 s in methanol. Insert a indicates fit of abs vs time data to first-order exponential at 320 nm.

spectrophotometer. It was thus confirmed from all kinetics experiments that only one reaction (i.e., coordinated methanol substitution) took place for all the metal complexes and with all the relative entering ligands used, as illustrated by the formation of isosbestic points observed with successive abs vs wavelength scans, as per example in Figure 3.

As stated above, the rates and concentration dependences obtained in this study therefore assumed that the aqua complexes, immediately upon dissolution in methanol, exchanges the coordinated aqua to form the corresponding solvated *fac*-$[Re(CO)_3(L,L'\text{-Bid})(MeOH)]^n$ complexes. The synthesis of **3** from solutions of **4** and Br^- ions also provide proof for the absence of complicated side processes in these coordinated methanol substitution reactions.

The coordinated methanol substitution in **1b** and **2b** (*N,N'*-Bid), **4b** and **5b**, **10b** and **11b** (*N,O*-Bid), and **7b** and **8b** (*O,O'*-Bid) (**a** suffixes indicate the corresponding *aqua* complexes, while **b** suffixes indicate the coordinated *methanol* rhenium(I) complexes of **1**, **2**, **4**, **5**, **7**, **9**, **10**, and **11**, respectively) was investigated and analyzed for a range of entering ligands. Figure 3 shows an example of the typical time-resolved absorbance change scan, which has typically been observed for all substitution reactions in this study. Time-resolved absorbance change values may then be fitted to single exponentials (insert a in Figure 3), confirming first-order behavior. All subsequent plots of k_{obs} versus ligand concentration yielded straight lines and the data was fitted to eq 2 using linear least-squares fits.[53] Figure 4 gives a representative illustration and summary of some reaction plots for the range of different complexes and entering ligands.

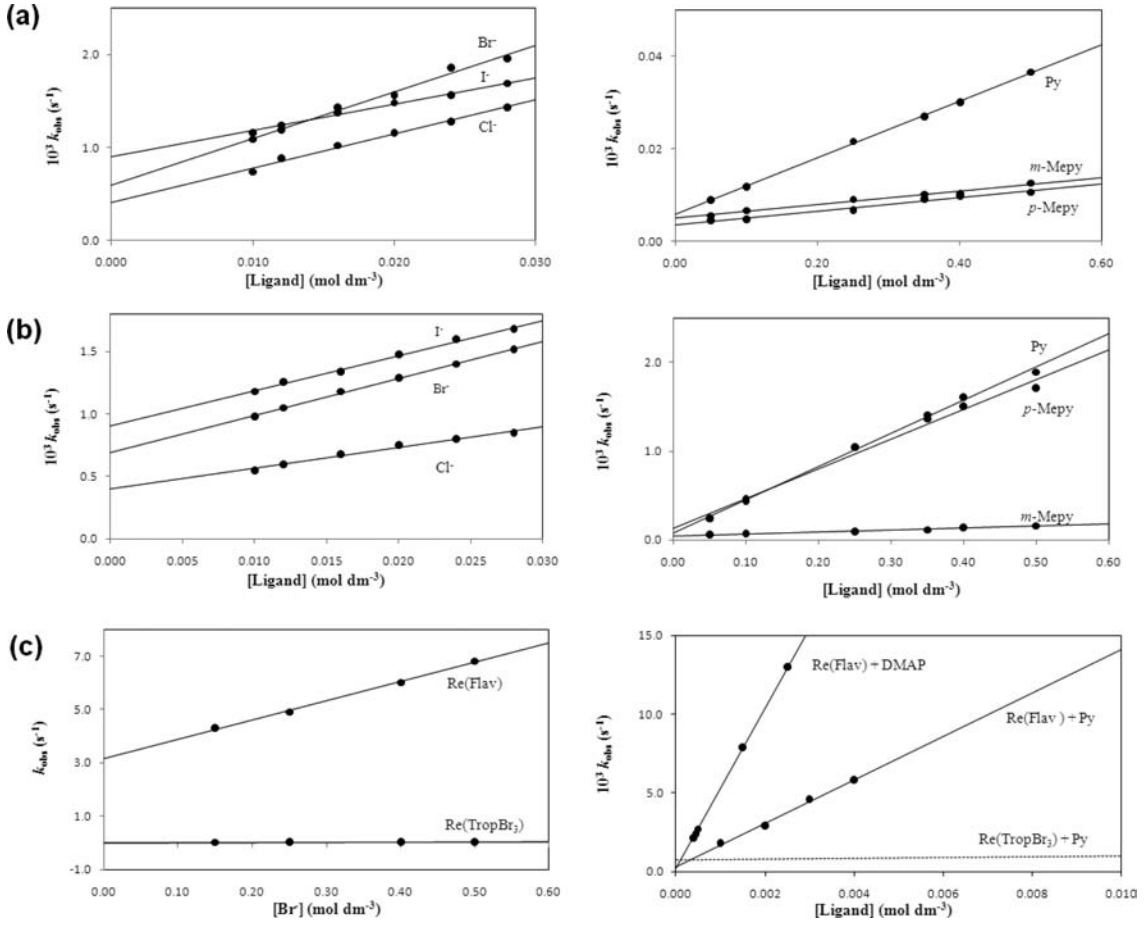

Figure 4. Selected plots of k_{obs} vs entering ligand concentration for the reactions of *N,O*- and *O,O'*-Bidentate ligand rhenium(I) complexes: (a) *fac*-$[Re(CO)_3(Phen)(MeOH)]^+$ **2b**, (b) *fac*-$[Re(CO)_3(Quin)(MeOH)]$ (**11b**), and (c) *fac*-$[Re(CO)_3(TropBr_3)(MeOH)]$ (**7b**) and *fac*-$[Re(CO)_3(Flav)(MeOH)]$ (**8b**) with different entering ligands in methanol at 25.0 °C.

dx.doi.org/10.1021/ic2013792 | *Inorg. Chem.* 2011, 50, 12486–12498

The kinetics of the substitution of the coordinated aqua ligand in a range of *fac*-tricarbonyl rhenium(I) complexes containing a range of *N,N′*-, *N,O*-, and *O,O′*-donor bidentate ligands have thus been studied and the results are stepwise reported below.

***N,N′*-Bidentate Ligands.** The rates of coordinated methanol substitution in **1b** and **2b** were monitored by UV−vis spectroscopy at 25.0 °C and 340 nm. The entering ligands used in this part of the study were halides (Cl^-, Br^-, I^-), pyridine type ligands (pyridine, *meta*-, and *para*-methylpyridine (*m*-Mepy and *p*-Mepy)), 1,3,5-Triaza-7-phosphadamantane (PTA),[57,58] a water-soluble phosphine ligand, and methylurea (Metu) as a S-donating ligand. All the reactions were performed under pseudo-first-order reaction conditions with the entering ligand in excess. The rate and equilibrium constants for these reactions are reported in Table 4 and the data fits of *fac*-$[Re(CO)_3(Phen)(MeOH)]^+$ (**2b**) are presented in Figure 4. Eyring plots for a selection of these processes yielded the activation parameters, which are reported later.

***N,O*-Bidentate Ligands.** The coordinated methanol substitution reactions of **4b** with bromide ions (Br^-), pyridine (Py), pyrazole (Pz), imidazole (Im), and 4-dimethylamino pyridine (DMAP) in methanol were monitored at temperatures ranging from 15.0 to 45.0 °C. These rate constants with various entering ligands are presented in Table 5 as well as that for the related compounds *fac*-$[Re(CO)_3(Pico)(MeOH)]$[46] **10b** and *fac*-$[Re(CO)_3(Quin)(MeOH)]$ **11b**.[45] The data for the reactions of **5b** with Py and DMAP at 25.0 °C are also presented in Table 5, while an illustrative plot of k_{obs} versus [ligand] for **11b** with different ligands is given in Figure 4(b).

Figure 5 gives a plot of $\ln(k/T)$ vs $1/T$ for the reactions of **4b** and *fac*-$[Re(CO)_3(Pico)(MeOH)]$ with the respective entering ligands. The activation parameters for **4b** and **7b** were obtained from similar Eyring plots and are reported in Table 6. Selective data for systems as indicated in Table 6 have been also analyzed with a global fit utilizing all the individual k_{obs} versus [L] versus temperature data points. It is clear that the traditional Eyring plots yielded similar results and do not influence conclusions made.

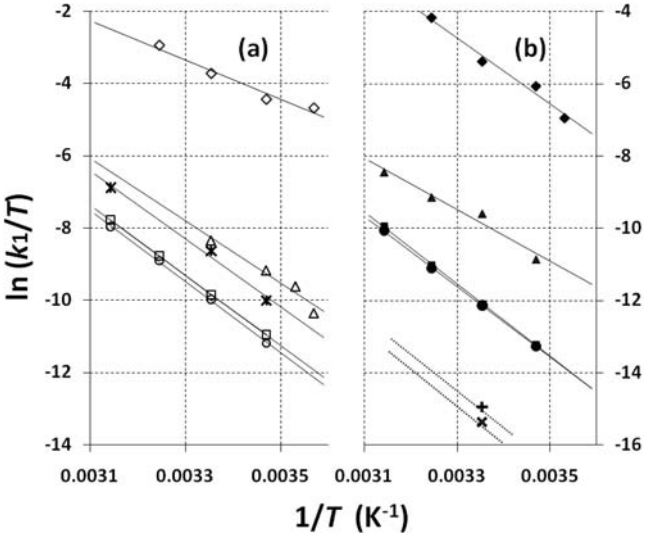

Figure 5. Eyring plots $[\ln(k_1/T)$ vs $1/T]$ for the reaction of entering entering ligands (a) *halides* (I^- or Br^-) compared to (b) *pyridine*; with different renium(I) metal complexes, indicated as [Complex] (L; symbol): *fac*-$[Re(CO)_3(bipy)(MeOH)]^+$ **1b**, (py, +); *fac*-$[Re(CO)_3(Phen)(MeOH)]^+$ **2b**, (I^-, ∗; py, ×); *fac*-$[Re(CO)_3(2,4\text{-}dPicoH)(MeOH)]$ **4b**, (Br^-, □; py, ■); *fac*-$[Re(CO)_3(TropBr_3)(MeOH)]$ **7b**, (Br^-, Δ; py, ▲); *fac*-$[Re(CO)_3(Flav)(MeOH)]$ **9a**, (Br^-, ◇; py, ◆); and *fac*-$[Re(CO)_3(Pico)(MeOH)]$ **10b**, (I^-, ○; py, ●).

***O,O′*-Bidentate Ligands.** The reactions of *fac*-$[Re(CO)_3(TropBr_3)(MeOH)]$ (**7b**) and *fac*-$[Re(CO)_3(Flav)(MeOH)]$ (**9a**) with pyridine and 4-dimethylaminopyridine were performed at 15.0, 25.0, 35.0, and 45.0 °C (see Supporting Information for the relevant rate data). Selective data for k_{obs} versus [ligand] for **7b** and **9a** with py and DMAP is illustrated in Figure 4(c) and reported in Table 5, while the activation parameters for **7b** and **9a** with Br^-, py and DMAP as entering ligands were obtained from Eyring plots and are reported in Table 6.

DISCUSSION

Synthesis. The synthesis proved to be simple once the basic behavior of these systems have been quantified, and in general the aqua species could be obtained in high yields provided that cognizance of the kinetics of the fairly slow halide abstraction is taken into account. Sufficient time, that is, ∼12 h, should be allowed for this, which is in agreement with the acid hydrolysis/solvolysis rate as obtained from the anation reactions with bromide ions, that is, k_{-1} values of $<1 \times 10^{-4}$ s^{-1}, with half-lives of a few hours.[29]

X-ray Crystallography. All four compounds **2**, **5**, **6**, and **9** crystallize in either triclinic or monoclinic space groups with the respective asymmetric units consisting of one parent molecular compound and various solvate and non coordinating ligands. These are briefly described as follows: the asymmetric unit in **2** is characterized by a *fac*-$[Re(CO)_3(Phen)(H_2O)]^+$ cation (**2a**), a nitrate anion and half of a noncoordinating Phen molecule; **5** consists of *fac*-$[Re(CO)_3(2,4\text{-}dQuinH)(H_2O)]$ (**5a**) and one aqua solvate molecule; **6** consists of *fac*-$[Re(CO)_3(2,4\text{-}dQuinH)Py]$ (**6a**) and a noncoordinating pyridine molecule while **9** consists of a *fac*-$[Re(CO)_3(Flav)(CH_3OH)]$ (**9a**) and one CH_3OH solvate molecule. In general, for all the structures presented here, the coordination geometery around the Re atom is a distorted octahedron consisting of the bidentate ligand, three facial carbonyl ligands and either a water molecule (**2** and **5**), a pyridine ligand (**6**) or a CH_3OH ligand (**9**).

The Re−N bond distances [(**2**) 2.168(4) − 2.174(4) Å; (**5**) 2.220(5) Å; (**6**) 2.247(3) Å] compare well with that found for other complexes.[59] The N−Re−N angle of 75.86(15)° in **2** is also consistent with other structures and probably is the main reason for the octahedral distortion around the Re(I) center. The Re−O (bidentate ligand) bond distances in **9** are 2.147(3) and 2.143(3) Å, also comparing well with known complexes with *O,O′*-bidentate ligands and the Re−O distances obtained for **5** and **6**. The Re−OH_2 bond distances are of most interest here and were recorded as 2.162(3) Å for (**2**) and 2.182(4) for (**5**) respectively. These compare well with the similar bonds in structural reports of *fac*-$[Re(CO)_3(L,L'\text{-}Bid)(H_2O)]^n$ (*L,L′*-Bid = *N,N′*-donor atom bidentate ligands)[13,30] but are slightly shorter than the Re−O bond distances in *fac*-$[Re(CO)_3(H_2O)_3]^+$ (2.201(14) Å).[34]

The bite angles formed by the bidentate ligands and the Re(I) metal are comparable for all the complexes (N−Re−N 75.86(15)° for **2**, N−Re−O angles of 75.25(15)° and 75.679(13) ° for **5** and **6**, respectively, and the O−Re−O angle of 76.24(11)° for **9**). This probably means that any bond lengthening observed in the Re−OH_2 bonds could be

dx.doi.org/10.1021/ic2013792 | *Inorg. Chem.* 2011, 50, 12486−12498

Table 6. Activation Parameters for the Anation/Coordinated Methanol Substitution in *fac*-[Re(CO)$_3$(*L,L'*-Bid)(MeOH)]^n Complexes with Different Entering Ligands in Methanol at 25.0 °C

	10^3 k_1 ($M^{-1}s^{-1}$)	10^3 k_{-1} (s^{-1})	K_1[a] (M^{-1})	$\Delta H^{\ddagger}$ (kJ mol^{-1})	$\Delta S^{\ddagger}$ (J K^{-1} mol^{-1})	$\Delta G^{\ddagger}_{298}$ (kJ mol^{-1})
			[Re(CO)$_3$(Phen)(MeOH)]$^+$ (**2b**)			
I^-	53(1)	0.7(1)	76(11)	70(1)	−35(3)	80(2)
Metu	13.7(1)	0.011(1)	1245(114)	80(1)	−9(3)	83(2)
				79(1) [b]	−10(2) [b]	82(2)
			[Re(CO)$_3$(2,4-dPicoH)(MeOH)] (**4b**)			
Br^-	15.7(2)	0.63(8)	25(3)	80.8(6)	−8(2)	82(1)
				79(1) [b]	−8(4) [b]	81(1)
Py	1.641(8)	0.030(2)	21(1)	84(2)	−19(4)	90(3)
Pz	2.336(9)	0.016(3)	146(27)	83(1)	−18(3)	88(2)
Im	1.44(4)	0.070(5)	21(2)	85.2(7)	−13(2)	89(1)
DMAP	3.21(4)	0.11(1)	29(3)	84.3(3)	−10(1)	87(1)
			[Re(CO)$_3$(Pico)(MeOH)] (**11b**)			
I^-	14(1)	0.64(1)	22(2)	77(1)	−19(3)	83(2)
Py	1.6(1)	0.0084(1)	190(12)	84(1)	−16(4)	89(2)
			[Re(CO)$_3$(TropBr$_3$)(MeOH)] (**7b**)			
Br^-	70.6(4)	4(1)	18(4)	63(6)	−54(19)	79(6)
Py	20.3(7)	1.6(2)	13(2)	53(5)	−102(17)	83(6)
				45(5)[b]	−122(15) [b]	81(6)
DMAP	34.5(7)	0.26(2)	133(11)	69(4)	−42(12)	82(5)
			[Re(CO)$_3$(Flav)(MeOH)] (**9a**)			
Br^-	7.2(3) × 10^3	3.17(9) × 10^3	2.5(2)	52(5)	−52(15)	67(6)
Py	1.38(8) × 10^3	0.3(1)	4.6(1) × 10^3	54(6)	−60(21)	72(6)
DMAP	5.1(2) × 10^3	0.16(4)	3.2(8) × 10^4	84(4)	51(14)	69(5)

[a] $K_1 = k_1/k_{-1}$; eq 1. [b] Activation parameters from global fits.

attributed to the electronic effects of the bidentate ligand and that such bond lengthening in the solid state could potentially be observed in the substitution kinetics.

All the structures exhibit extensive hydrogen bonding networks (see Supporting Information) with the solvent molecules or cocrystallizing ligands serving as links between the metal compounds. π-Stacking, with a centroid to centroid distance of 3.611 Å is observed in **9** between both the A ring of one bonded flavone ligand and a neighboring C ring of the next molecular compound and vice versa.

UV−vis Spectroscopy. The different complexes show typical UV−vis spectra the low-spin d^6 metal Re(I) center under the influence of the strong ligand field affected by the *fac*-tricarbonyl orientation, and once ligand substitution have been affected, typical UV−vis transitions are observed.[60]

The UV−vis data indicate that the transitions and molar extinction coefficients vary in a systematic way, see Table 3. The six aqua complexes however do not show a systematic change upon variation of the *L,L'*-Bid ligands. There is more pronounced batochromic shift for the *N,N'*-Bid systems for the halides compared to the pyridine-type ligands, in agreement with the stability constants of these complexes. The effect for the *N,O*- and *O,O'*-Bid complexes is also not systematic, although the intensity of the bands vary significantly by ∼1 order of magnitude from ∼4000−8000 M^{-1} cm^{-1} for the Bipy/Phen complexes to ∼12000−25000 M^{-1} cm^{-1} for the $TropBr_3^-$/$Flav^-$ to ∼40000−50000 M^{-1} cm^{-1} for the 2,4-$dPicoH^-$ complexes, suggesting a more significant influence on the crystal field energies induced to the rhenium center by the negatively charged *N,O*- and *O,O'*-Bid ligands compared to that of the neutral *N,N'*-Bid ligands.

IR Spectroscopy. The IR data as reported in Table 3 indicate that the symmetric stretching bands (terminology defined based on assuming the two CO ligands to be equivalent, that is, vibration because of simultaneous bond stretching) from the carbonyl ligands show a progressive decrease in wavenumber for the aqua complexes as follows:

(i) *fac*-[Re(CO)$_3$(*L,L'*-Bid)(H$_2$O)]^n: For *L,L'*-Bid: 2,4-$dPicoH^-$ and 2,4-$dQuinH^-$ 2035 and 2034; $TropBr_3^-$, $Pico^-$ and $Quin^-$ 2024, 2022, and 2018, $Flav^-$ 2013; and Bipy and Phen both 2008 cm^{-1}, respectively. Thus, a total progressive decrease of ∼20 cm^{-1} is observed.

(ii) *fac*-[Re(CO)$_3$(*L,L'*-Bid)(Br)]^n: A similar but less significant decrease is observed: ∼20 cm^{-1} for 2,4-$PicoH^-$ and 2,4-$QuinH^-$, 2021 and 2020, $TropBr_3^-$ 2008 and $Flav^-$ 1999 cm^{-1}.

(iii) *fac*-[Re(CO)$_3$(*L,L'*-Bid)(py)]^n: A similar but less significant decrease is observed: ∼15 cm^{-1} for 2,4-$PicoH^-$ and 2,4-$QuinH^-$, 2029 and 2024, $TropBr_3^-$ 2015 and $Flav^-$ 2012 cm^{-1}.

(iv) For every *L,L'*-Bid ligand system, there is a clear decrease of ∼10 cm^{-1} from the aqua > py-type > Br^- complexes, in agreement with the ligand strength.[59]

The above is indicative of a parallel increase in electron density on the metal center due to the *L,L'*-Bid ligand interaction of the aqua and substituted complexes as the π-backbonding into the CO antibonding orbitals increase. The increased electron density introduced by the ligands manifests itself in the concurrent increased softness of the metal center, in agreement with examples from literature.[61−64] Smaller changes are observed in the asymmetric stretching bands, with no clear tendency and further interpretation is currently not attempted.

Stability Constants. The stability constants K_1 for the ligation reaction in eq 1 are listed in Tables 4 and 5, and there is a reasonable to good agreement of the kinetically vs. thermodynamically determined values. In general, the indication is that

dx.doi.org/10.1021/ic2013792 | Inorg. Chem. 2011, 50, 12486−12498

there is an under estimation in the k_{-1} values, resulting in a corresponding over estimation of the stability constants. Nevertheless, there is a progressive change in the stability constants K_1 of all the *fac*-$[Re(CO)_3(L,L'\text{-Bid})(X)]^n$ complexes as follows: *N,N'*-Bid, halides ≅ PTA, Tu > py-type ligands; while for the *N,O*-Bid: halides < py-type ligands and *O,O'*-Bid: halides ≪ py-type ligands. For the cationic complexes phen and bipy, the halido complexes are approximately one order-of-magnitude larger when compared to the corresponding pyridine complexes. This changes to similar stabilities for the halido and pyridines in the *N,O*-Bid complexes, but is switched around in the *O,O'*-Bid complexes, that is, the halido complexes are approximately one order-of-magnitude less stable than the corresponding pyridine complexes. This is a manifestation of the increased electron density on the metal center when progressing from the *N,N'*- to *N,O*- to finally the *O,O'*-Bid complexes.

Substitution Kinetics. Solutions of selected complexes, that is, **1b**, **2b**, **10b**, and **11b** (*fac*-$[Re(CO)_3(L,L'\text{-Bid})(MeOH)]^n$ with *L,L'*-Bid = Bipy, Phen, Pico$^-$ and Quin$^-$ respectively, see also below), in water and also in water/methanol remained stable for days, confirming that the reverse reaction is slow and not that pronounced given the correct choice of ligand concentration ranges.

***N,N'*-Bid Ligands.** It is evident from Table 4 that the rates of formation, k_1, for the halides (Cl^-, Br^-, and I^-) as entering ligands are comparable for the reactions of **1b** and **2b** and that these rate constants are in general 300−400 times faster than the values obtained for the neutral pyridine type ligands, about 4 times faster than the values calculated for PTA and only twice as fast as the values obtained for Metu. On face value, the higher affinity of the positively charged metal complex for the negatively charged entering halide ions indicates an associative mode of activation.

The k_1 values obtained for the reactions of **1b** and **2b** with Py and *m*Mepy also needs mentioning. It seems that the more sterically hindered *m*Mepy reacts 4−6 times slower than its unsubstituted counterpart (0.096(1) and 0.064(3) × 10^{-3} M^{-1} s^{-1} compared to 0.028(1) and 0.014(1) × 10^{-3} M^{-1} s^{-1}, respectively). However, a similar decrease is observed for pMepy, which has no net steric demand when compared to pyridine. This cannot be explained currently.

This large variation of k_1 with the type of entering ligand was not observed for the substitution reactions of *fac*-$[Re(CO)_3(H_2O)_3]^+$ where an I_d type mechanism was proposed for these reactions. These conclusions were also confirmed with high-pressure studies[29] and the fact that the rate constants of the reverse reactions showed considerable variation. Salignac and co-workers[13] obtained a value of 1.6(3) × 10^{-3} M^{-1} s^{-1} for the formation of *fac*-$[Re(CO)_3(H_2O)_2Br]$. This is about 20 to 30 times slower than the similar reactions observed here for **1b** and **2b** with Br^- ions. This increase in rate for the reactions of **1b** and **2b** is carried through for all the N and S donor type ligands used in this study compared to those used by Salignac et al. This is an indication of the ability of Bipy and Phen to activate the metal complex and thereby increase the rate of anation.

The values for the reverse reactions, k_{-1}, show a variation of only a hundred times as opposed to the six thousand times variation for the k_1. This also indicates toward an I_a mechanism.

The largest differences in forward rate constants, k_1, for the reactions of **1b** and **2b** are observed between I^- and *m*Mepy as entering ligands where variations of almost 2000 times for **1b** and almost 4500 times for **2b** were obtained.

High pressure studies of Alberto co-workers[29] on the formation of monosubstituted products indicated a mechanistic changeover from I_d for harder N donor to I_a for the softer S donor ligands. This, together with the fact that the three successive reactions observed for *fac*-$[Re(CO)_3(H_2O)_3]^+$ and DMS (dimethyl sulfide) showed a decrease in formation rates when moving from the mono- to the di- and trisubstitution products, related to the increased steric hindrance on the metal center, and providing some evidence for the proposed I_a mechanism.

***N,O*-Bid Ligands.** It is clear from Table 5 that k_1 for the reactions of **4a** with Br^- as entering ligand is ∼5−7 times faster at 25.0 °C than what was found for the neutral ligands. In terms of the neutral ligands, k_1 (DMAP) is only slightly larger than the other rate constants. This is expected for an associative activated mechanism since the pK_a of DMAP (9.8) is higher than that of imidazole (6.99), pyridine (5.25), and pyrazole (2.49).[65] However, the absence of a significant increase suggests that association does not play that important part in the mechanism. The negative values obtained for $\Delta S^{\ddagger}$ however point to an I_a type mechanism. The values of k_1 for the reactions of **5b** with Py and DMAP are comparable to the similar reactions of these ligands with **4b** as expected.

Interesting observations are made from the comparison of the forward rate constants, k_1, for reactions of **4b** and **5b** with the similar reactions of **1b** and **2b**. For the reactions with Br^-, k_1 for the positively charged **1b** and **2b** are about 3 to 4 times faster than for the neutral **4b**. This observation is significantly reversed when the rate constants of **1b** and **2b** are compared with **4b** and **5b** for the reactions with Py. The largest increase is observed between **5b** (3.31(2) × 10^{-3} M^{-1} s^{-1}) and **2b** (0.064(3) × 10^{-3} M^{-1} s^{-1}), a difference of almost 50 times. This observation is curious since, all other things being equal, one would expect the more positively charged complexes to be more reactive toward substitution in purely associative activated reactions. This points toward an I_d mechanism for the neutral complexes.

The effect of the additional carboxylate group on the reactivity of both the pico$^-$ and quin$^-$ backbones proved to be fairly negligible, as manifested in the comparison of the k_1 values of the pairs **4b**/**10b**, and **5b**/**11b**, see Table 5, in spite of significant ligand field influences observed due to assumed electron delocalization.

***O,O'*-Bid Ligands.** The data in Table 5 indicate that the value of k_1 obtained for the reaction between **8b** and DMAP is almost 150 times faster than that with **7b**. This could possibly be due to the electron withdrawing effects of the bromide substituents on $TropBr_3$. One would expect the $Flav^-$ ligand to have better electron donating ability when compared to $TropBr_3^-$, although this ground state destabilization was not observed in the solid state (crystallographic study) where the Re to *O,O'*-Bid bond distances were similar for **9** and *fac*-$[Re(CO)_3(TropBr_3)Br]$.[56] For the neutral aqua complexes (**4b**, **5b**, **7b**, and **9a**), the ν_{co} data indicate that the Re−OH_2 bond is weakened in the series: **4b** ≈ **5b** < **7b** < **9a**, and this is reflected in the rate constant data with k_1 for **9a** being the largest in each case. The labilizing effect of $Flav^-$ may be illustrated by the comparative values for k_1 for **9a** and **2b** at 25.0 °C and with Py as entering ligand where an increase of >4 orders of magnitude was observed.

This is further illustrated by the Eyring plots in Figure 5. In fact, if the transition from the pure *fac*-triaqua complexes from Grundler is considered,[28,29] an activation of more than *5 orders-of-magnitude* (4 × 10^5) is observed from two aqua equatorial ligands compared to having $Flav^-$ as *O,O'*-Bid ligand.

dx.doi.org/10.1021/ic2013792 | *Inorg. Chem.* 2011, 50, 12486−12498

Significant increase of electron density on the metal center clearly will promote an increase in the rate of all the entering ligands studied for the *O,O′*-Bid ligands compared to the *N,O*- and the *N,N′*-Bid ligands agreement with the IR data. This clearly indicate that the dissociation of the coordinated methanol is more important in the electron rich *fac*-[Re(CO)$_3$(*O,O′*-Bid)(MeOH)] complexes. For a pure associative mechanism, the significant increase in formation rate constants for these complexes is not expected. In fact, the opposite is true, that is, the rate constants should decrease.

In summary, the following can be highlighted: The coordinated methanol substitution reactions between the Re(I) complexes **1b**, **2b**, **4b**, **5b**, **7b**, **9a**, **10b**, and **11b** and various entering nucleophiles were investigated. From this data it was observed that the first-order rate constants, k_1, decrease in general for Br^- > DMAP > Py, Pz, Im. This decrease is generally consistent with the nuceophilicity of the entering ligands as illustrated by its pK_a values and supports an associative activated type mechanism for these reactions. The negative values obtained for $\Delta S^{\ddagger}$ also support this observation.

■ ACTIVATION PARAMETERS

The activation parameters in Table 6 indicate that the substitution process of the *fac*-[Re(CO)$_3$(*L,L′*-Bid)(MeOH)]^n complexes most likely proceed via an interchange mechanism, with the cationic bipy and phen and complexes leaning toward I_a, while the neutral complexes of *N,O*- and *O,O′*-Bid might suggest an I_d mechanism.

Upon superficial consideration of the results from the Eyring plots, two approximate zones for the activation parameters are observed. First, the *N,N′*- and *N,O*-Bid complexes show less than 10% contributions [excluding the reaction between *fac*-[Re(CO)$_3$(Phen)(MeOH)]$^+$ **2b**, and iodide ions ($\Delta S^{\ddagger}(I^-)$ = −35(3) J K^{-1} mol^{-1}), which might suggest a more associative activation because of Coulombic contributions by two oppositely charged species] to $\Delta G^{\ddagger}_{298}$ by the entropic terms, that is, the transition states are primarily dependent on bond breaking/formation rather that ordering. Second, in the case of the *O,O′*-Bid ligands, however, the entropy contribution to $\Delta G^{\ddagger}_{298}$ increases to 20−40%, seemingly indicting more order in the activation step. However, upon carefully considering the uncertainties in the entropy of activation, it is clear that the *O,O′*-Bid ligand values are comparable with the *N,N*- and *N,O*-Bid systems, and therefore does not provide conclusive evidence. Moreover, a postitive value of +52(14) J K mol is observed for $Flav^-$, which might indicate a more dissociative activation.

■ CONCLUSIONS

The effects of different bidentate donor ligands on the reactivity of the Re(I) metal center were illustrated by use of *N,N′*-, *N,O*-, and *O,O′*-Bid ligands. A general trend of k_1 for the Re(I) complexes defined in **9a** > **7b** > **5b** > **4b** > **11b** > **10b** > **2b** > **1b** > **0b** (see below) was observed and is similar to the trend observed for ν_{co} for these Re(I)-MeOH complexes.

Salignac and co-workers obtained a value of 1.6(3) × 10^{-3} M^{-1} s^{-1} for the formation of *fac*-[Re(CO)$_3$(H$_2$O)$_2$Br]. This is about 20 - 30 times slower than the similar reactions observed here for **1b** and **2b** with Br^- ions, where two aqua ligands are replaced by an *L,L′*-Bid ligand, underlining the weak "cis" effect by two water molecules.

It was concluded that the *O,O′*-Bid type donor ligands utilized here activate the metal center substantially more than the *N,O*-Bid type ones and that positively charged complexes have slower coordinated methanol substitution rates. More data and a wider range of complexes may have to be investigated in future studies to gain a better understanding of the intimate mechanism of these reactions. The fact that **8a** undergoes much faster coordinated methanol substitution reactions could prove an important observation to be exploited in future studies, having for example, a biologically active ligand so close to the metal center might have some advantages in terms of radiopharmacy. Furthermore the high stability constants, K_1, observed for the reactions of **8a** with DMAP and Py suggests a significant increased stability when incorporating a single pyridine based monodentate ligand in the apical H$_2$O/methanol site in combination with a biological-type *O,O′*-Bid flavanoid type bidentate chelate.

The greater significance of our results is that bidentate ligands can labilize the metal center and that this study should be further expanded to explore other ligand systems, but even more significant is the increased affinity of Re(I) for hard nucleophiles like pyridine, indicitave of the influence of the bidentate ligands. Finally, it underlines the fact that the potential use of bidentate ligands in a typical [2 + 1] mixed ligand approach may significantly affect the "labile site", thus governing the reactivity and stability of the "1-site", and cannot be ignored when designing and evaluating new agents. The kinetic data presented also enabled the stability constants for the substituted products to be estimated for a range of bidentate/monodentate combinations which allows prediction of reactivities/stabilities of similar [2 + 1] complexes to be evaluated in future.

■ ASSOCIATED CONTENT

Ⓢ Supporting Information

CCDC 815753, 815750, 815751, and 815752 contains the supplementary crystallographic data for **2**, **5**, **6**, and **9**. This data can be obtained free of charge from The Cambridge Crystallographic Data Centre via www.ccdc.cam.ac.uk/data_request/cif. Structural data for the complex fac-[Re(CO)$_3$(Bipy)Br], All the kinetic data, including k_{obs} values and temperature studies for the complexes of **1b** and **2b**, and that for complexes **4b**, **5b**, **10b**, and **11b** and for complexes **7b** and **8b**. This material is available free of charge via the Internet at http://pubs.acs.org.

■ AUTHOR INFORMATION

Corresponding Author

*E-mail: visserhg@ufs.ac.za (H.G.V.); roodta@ufs.ac.za (A.R.).

■ ACKNOWLEDGMENTS

We would like to thank Dr. Inus Janse van Rensburg, Dr. Fanie Muller, and Mr. Leo Kirsten for the crystal data collections. Financial assistance from the University of the Free State is gratefully acknowledged. We also express our gratitude towards SASOL, PETLabs Pharmaceuticals, the South African National Research Foundation (SA-NRF/THRIP) and the University of the Free State Strategic Academic Initiative (Advanced Biomolecular Cluster) and the University of Johannesburg for financial support of this project. The University of the Witwatersrand (Prof. Dave Billing) is also acknowledged for the use of their diffractometer. Opinions, findings, conclusions

or recommendations expressed in this material are those of the authors and do not necessarily reflect the views of the SA NRF.

REFERENCES

(1) Zobi, F.; Blacque., O.; Sigel, R. K. O.; Alberto, R. *Inorg. Chem.* **2007**, *46*, 10458−0460.
(2) Spingler, B.; Mundwiler, S.; Ruiz-Sanchez, P.; van Staveren, D. R.; Alberto, R. *Eur. Jour. Inorg. Chem.* **2007**, *18*, 2641−2647.
(3) Alberto, R.; Schibli, R.; Schubiger, P. A.; Abram, U.; Kaden, T. A. *Polyhedron* **1996**, *15*, 1079−1089.
(4) Alberto, R.; Schibli, R.; Waibel, R.; Abram, U.; Schubiger, A. P. *Coord. Chem. Rev.* **1999**, *192*, 901−919.
(5) Abram, U.; Abram, S.; Alberto, R.; Schibli, R. *Inorg. Chim. Acta* **1996**, *248*, 193−202.
(6) Alberto, R.; Herrmann, W. A.; Kiprof, P.; Baumgärtner, F. *Inorg. Chem.* **1992**, *31*, 895−899.
(7) Castro, H. H. K.; Hissink, C. E.; Teuben, H. J. H.; Vaalburg, W.; Panek, K. *Recl. Trav. Chim. Pays-Bas.* **1992**, *111*, 105−108.
(8) Alberto, R.; Schibli, R.; Abram, U.; Egli, A.; Knapp, F. F.; Schubiger, P. A. *Radiochim. Acta.* **1997**, *79*, 99−103.
(9) Schibli, R.; Alberto, R.; Abram, U.; Abram, S.; Egli, A.; Schubiger, P. A.; Kaden, T. A. *Inorg. Chem.* **1998**, *37*, 3509−3516.
(10) Alberto, R.; Egli, A.; Schibli, R.; Abram, U.; Kaden, T. A.; Schaffland, A. O.; Schwarzbath, R.; Schubiger, P. A. *Q. J. Nucl. Med.* **1998**, *42* (suppl), 9.
(11) Alberto, R.; Schibli, R.; Egli, A.; Schubiger, P. A.; Herrmann, W. A.; Artus, G.; Abram, U.; Kaden, T. A. *J. Organomet. Chem.* **1995**, *493*, 119−127.
(12) Booysen, I. N.; Gerber, T. I. A.; Mayer, P. *Inorg. Chim. Acta* **2010**, *363*, 1292−1296.
(13) Salignac, B.; Grundler, P. V.; Cayemittes, S.; Frey, U.; Scopelliti, R.; Merbach, A. *Inorg. Chem.* **2003**, *42*, 3516−3526.
(14) Leipoldt, J. G.; Basson, S. S.; Roodt, A. *Adances in Inorganic Chemistry*; Sykes, A. G., Ed; Academic Press: New York, 1993; Vol *40*, p 297.
(15) Roodt, A.; Abou-Hamdan, A.; Engelbrecht, H. P.; Merbach, A. E. *Advances in Inorganic Chemistry*; Sykes, A. G., Ed; Academic Press: New York, 2000; Vol *49*, p 59.
(16) Engelbrecht, H. P.; den Drijver, L.; Steyl, G.; Roodt, A. *C. R. Chim.* **2005**, *8*, 1660−1669.
(17) Engelbrecht, H. P.; Jurisson, S. S.; Cutler, C. S.; den Drijver, L.; Roodt, A. *Synth. React. Inorg. Met.-Org. Nano-Met. Chem.* **2005**, 83−90.
(18) Roodt, A.; Engelbrecht, H. P.; Botha, J. M.; Otto, S. *Technetium, Rhenium and Other Metals in Chemistry and Nuclear Medicine*; Nicolini, M., Mazzi, U., Eds; S G Ed.ial Publishers: Padova, Italy, 1999; Vol *5*, p 161.
(19) Roodt, A.; Botha, J. M. *Metal-Based Drugs* **2008**, No. 745989.
(20) Roodt, A.; Visser, H. G.; Brink, A. *Crystallogr. Rev.* **2011**, *17*, 241−280.
(21) Leipoldt, J. G.; Basson, S. S.; Roodt, A.; Purcell, W. *Polyhedron Rep. 44* **1992**, *11*, 2277−2283.
(22) Roodt, A.; Leipoldt, J. G.; Helm, L.; Merbach, A. E. *Inorg. Chem.* **1994**, *33*, 140−147.
(23) Abou-Hamdan, A.; Roodt, A.; Merbach, A. E. *Inorg. Chem.* **1998**, *37*, 1278−1288.
(24) Leipoldt, J. G.; Basson, S. S.; Potgieter, I. M.; Roodt, A. *Inorg. Chem.* **1987**, *26*, 57−59.
(25) Roodt, A.; Leipoldt, J. G.; Deutsch, E. A.; Sullivan, J. C. *Inorg. Chem.* **1992**, *31*, 1080−1085.
(26) Roodt, A.; Leipoldt, J. G.; Helm, L.; Abou-Hamdan, A.; Merbach, A. E. *Inorg. Chem.* **1995**, *34*, 560−568.
(27) Zobi, F.; Blacque, O.; Steyl, G.; Spingler, B.; Alberto, R. *Inorg. Chem.* **2009**, *48*, 4963−4970.
(28) Grundler, P. V.; Helm, L.; Alberto, R.; Merbach, A. E. *Inorg. Chem.* **2006**, *45*, 10378−10390.
(29) Grundler, P. V.; Salignac, B.; Cayemittes, S.; Alberto, R.; Merbach, A. E. *Inorg. Chem.* **2004**, *43*, 865−873.
(30) Zobi, F.; Blacque, O.; Schmalle, H. W.; Spingler, B.; Alberto, R. *Inorg. Chem.* **2004**, *43* (6), 2087−2096.
(31) Mundwiler, S.; Kündig, M.; Ortner, K.; Alberto, R. *Dalton Trans.* **2004**, 1320−1328.
(32) Schutte, M.; Visser, H. G. *Acta Crystallogr.* **2008**, *E64*, m1226−m1227.
(33) Schutte, M.; Visser, H. G.; Roodt, A. *Acta Crystallogr.* **2008**, *E64*, m1610−m1611.
(34) Herrick, R. S.; Ziegler, C. J.; Cetin, A.; Franklin, B. R. *Eur. J. Inorg. Chem.* **2007**, 1632−1634.
(35) Mundwiler, S.; Kündig, M.; Ortner, K.; Alberto, R. *Dalton Trans.* **2004**, 1320−1328.
(36) Kotrl, S.; Sucha, L. *Handbook of Chemical Equilibrium in Analytical Chemistry*; Ellis Horwood Series in Analytical Chemistry; Ellis Horwood: Chichester, U.K., 1985.
(37) Jencks, W. P.; Westheimer, F. H. as reported by Williams, D. A. at http://www.cem.msu.edu/~reusch-/Virtual Text/acidity2/htm.
(38) Brown, H. C. In *Determination of Organic Structures by Physical Methods*;Braude, E. A, Nachod, F. C., Ed.; Academic Press: New York, 1955.
(39) Van der Westhuizen, H. J.; Meijboom, R.; Roodt, A.; Schutte, M. *Inorg. Chem.* **2010**, *49*, 9599−9608.
(40) Albert, A.; Philips, J. N. *J. Chem. Soc.* **1956**, 1294−1304.
(41) Bryson, A. *J. Am. Chem. Soc.* **1960**, *82*, 4558−4862.
(42) Strandjord, A. J. G; Smith, D. E.; Barbara, P. F. *J. Phys. Chem.* **1985**, *89*, 2365.
(43) Alberto, R.; Egli, A.; Abram, U.; Hegetschweiler, K.; Gramlich, V.; Schubiger, P. A. *J. Chem. Soc., Dalton Trans.* **1984**, 2815−2820.
(44) Schutte, M.; Visser, H. G.; Roodt, A. *Acta Crystallogr.* **2008**, *E64*, m1610−m1611.
(45) Kemp, G. PhD Thesis, University of Johannesburg, 2006.
(46) Schibli, R.; La Bella, R.; Alberto, R.; Garcia-Garayoa, E.; Ortner, K.; Abram, U.; Schubiger, P. A. *Bioconjugate Chem.* **2000**, *11*, 345−351.
(47) *SAINT-Plus*, version 6.02 (including XPREP); Bruker AXS, Inc.: Madison, WI, U.S.A., 1999.
(48) *SADABS*, version 2004/1; Bruker AXS, Inc.: Madison, WI, USA, 2004.
(49) Sheldrick, G. M. *SHELXL97*; University of Göttingen: Göttingen, Germany, 1997.
(50) Sheldrick, G. M. *Acta Crystallogr.* **2008**, *A64*, 112−122.
(51) Farrugia, L. J. *J. Appl. Crystallogr.* **1999**, *32*, 837−838.
(52) Brandenburg, K.; Putz, H. *DIAMOND*, release 3.1b; Crystal Impact GbR: Bonn, Germany, 2005.
(53) *Micromath Scientist for Windows*, version 2.01; MicroMath Inc.: St. Louis, MO, U.S.A., 1986−1995.
(54) Brink, A.; Visser, H. G.; Roodt, A. *J. Coord. Chem.* **2011**, *64*, 122−133.
(55) Schutte, M.; Visser, H. G.; Brink, A. *Acta Crystallogr.* **2009**, *E65*, m1575−m1576.
(56) Schutte, M.; Visser, H. G.; Steyl, G. *Acta Crystallogr.* **2007**, *E63*, m3195−m3196.
(57) Sam, Z.; Roodt, A.; Otto, S. *J. Coord. Chem.* **2006**, *59*, 1025−1036.
(58) Otto, S.; Roodt, A. *Inorg. Chem. Commun.* **2001**, *4*, 49−52.
(59) Wing Wa Yam, V.; Yang, Y.; Zhang, J.; Wai-Kin Chu, B.; Zhu, N. *Organometallics* **2001**, *20*, 4911−4918.
(60) Cotton, F. A.; Wilkinson, G.; Gaus, P. L. *Basic Inorganic Chemistry*, 3rd ed.; John Wiley & Sons Inc.: London, U.K., 1995.
(61) Crous, R.; Datt, M.; Foster, D.; Bennie, L.; Steenkamp, C.; Huyser, J.; Kirsten, L.; Steyl, G.; Roodt, A. *Dalton Trans.* **2005**, 1108−1116.
(62) Otto, S.; Roodt, A. *Inorg. Chim. Acta* **2004**, *357*, 1−10.
(63) Roodt, A.; Otto, S.; Steyl, G. *Coord. Chem. Rev.* **2003**, *245*, 125−142.
(64) Brink, A.; Visser, H. G.; Roodt, A.; Steyl, G. *Dalton Trans.* **2010**, *39*, 5572−5578.
(65) Perrin, D. D. *Dissociation Constants of Organic Bases in Aqueous Solution*; Butterworths: London, 1965; Supplement, 1972.